APPENDIX

NOTE: Nomenclature in this document follows the American Ornithological Society Check-list of North American Birds (https://americanornithology.org/publications/north-and-middle-american-checklist). Notably, the Little Auk (*Alle alle*) is referred to as Dovekie, and the Wilson's Storm Petrel (*Oceanites oceanicus*) is hyphenated as Wilson's Storm-Petrel.

DATA AVAILABILITY STATEMENT

All observational survey data are accessible via the Northwest Atlantic Seabird Catalog (O'Connell et al. 2009, Coleman et al. 2016), with the exception of Canadian data used in regional models, which were drawn from the Eastern Canada Seabirds at Sea database (Gjerdrum et al. 2012; accessible at https://open.canada.ca/data/en/dataset/f612e2b4-5c67-46dc-9a84-1154c649ab4e). Local digital aerial survey data are also accessible via OBIS-SEAMAP (Halpin et al. 2009; https://seamap.env.duke.edu/) under the dataset name "Digital video aerial surveys of seabirds and marine megafauna in the Gulf of Maine from May 2023 to January 2024".

Additional information about the regional models is available via Winship et al. (2023) at https://repository.library.noaa.gov/view/noaa/60582. Digital raster files with the regional model predictions are available from the Marine-life Data Analysis Team at https://seamap.env.duke.edu/models/mdat/avian.html. Additional information about the local digital aerial surveys is included in a report to the Bureau of Ocean Energy Management (BOEM) that will become publicly available following publication.

SUPPLEMENTARY METHODS

Gulf of Maine Surveys: Digital Aerial Survey Methods

Aerial survey data were collected using a digital video camera rig mounted on a fixed-wing twin engine aircraft with specific modifications for offshore survey operations. The camera rig housed four ultra-high-resolution digital video cameras (each camera is the equivalent of 16 x HD quality, which is effectively 4 x 4K resolution), using fast shutter speeds (more than 1/10,000th second) to allow videography at low light levels.

The survey aircraft flew at 220 km/hr (~120 kts) and at a height of approximately 400 m above sea level (ASL). With the camera sensor calibrated to a nominal ground sample distance (GSD) of 1.5 cm, each camera sampled a strip of 104 m width, separated from the next camera by ~17 m, thus providing a combined sampled width of 416 m within an overall strip width of 467 m.

The detection and analysis of objects in the survey footage employed a two-step process. Initially, trained reviewers located and marked objects found in the survey footage. Marked objects were then labelled with a group category, which includes birds, marine megafauna, or anthropogenic objects, such as vessels or buoys. At the survey speed and effective frame rate (~8 frames/s), each detection typically appeared across 6–8 consecutive frames, providing multiple perspectives to support confident identification and downstream measurement. A 'blind' review of 20% of the imagery was performed and the results compared with those of the original object detection review. If 90% agreement was not attained during this process, then corrective action was initiated: that is, the remaining data set was reviewed and if appropriate, the failed reviewer's data discarded and all data were re-reviewed.

A two-step process was also employed for the identification of objects marked in the survey footage. Objects marked by initial reviewers were reviewed and identified by a team of trained ornithologists and marine mammal specialists. Biota were identified to the lowest taxonomic level possible and assessed for any visible features that may indicate the age and/or sex of each animal, as well as any behavioral traits that could be gleaned from the imagery. All objects were assigned to a species group and, where possible, each of these was then further identified to species level. The species identifications were given a confidence rating of 'possible' (<50% certainty in the identification), 'probable' (50–95% certainty), or 'definite' (>95% certainty).

Any animal that could not be identified to species level was assigned to a 'No ID' category and only identified to a higher group level. If, on occasion, an unidentified animal was suspected to belong to two possible genera, then a broader group category was used. For example, a bird identified as a Manx Shearwater would usually be assigned to the group category 'Shearwater species', and a bird identified as a Common Murre to the group category 'Large Auk species'. However, if the bird had the potential to be either, then it would be assigned to a wider group category 'Shearwater/Auk species' and the species level recorded as 'No ID'. A 'blind' review of species identifications was performed by an external team of ornithologists and marine mammal specialists, and the results compared with those of the original identifications. This included the standard of 20% of all biota, plus 100% of all terns, shorebirds, *Pterodroma* petrels, and federally endangered species. Any disputed identifications were re-reviewed by a panel of specialists who made a final decision. If consensus could not be achieved, the external assessment was adopted as the final classification.

Gulf of Maine Surveys: Spatially-Explicit Abundance Estimator

We developed single-season density surface models (hereafter referred to as "seasonal DSMs") for bird species and species groups using sightings data from the 2023–24 Gulf of Maine digital aerial surveys. Surveys were conducted in only one month per season; therefore, seasons were

defined as spring = May, summer = August, autumn = October, and winter = January. We attempted to build a seasonal DSM for each species with at least 30 sightings in that season. Whenever possible, each seasonal DSM was based on data from only a single species. However, in a few instances, we pooled sightings of species or species groups with small sample sizes but similar ecological characteristics, and we built seasonal DSMs for the pooled taxa. To provide insight into spatiotemporal variability in the density of the entire bird community, we created seasonal DSMs for all bird sightings combined, including sightings that were not identified to species.

In the following sections, we describe the mathematical structure of the DSMs, model evaluation methods, and abundance prediction methods. All analyses were conducted using R version 4.4.2 (R Core Team 2024). DSMs were constructed using sdmTMB and sdmTMBextra (Anderson et al. 2024, Anderson 2025).

Gulf of Maine Surveys: Density Surface Model Structure

To construct each seasonal DSM, we related the number of birds sighted on a 4-km (2.16-NM) transect segment to three types of explanatory variables: (1) spatial coordinates; (2) dynamic environmental variables; and (3) static environmental variables.

The spatial component of each DSM was defined as one of two types of random effects: either (i) a stochastic partial differential equation (SPDE) approximation to model the precision matrix associated with the Matérn covariance function (i.e., an “SPDE Matérn model”; Lindgren et al. 2011); or (ii) an SPDE Matérn model that accounts for barriers (i.e., an “SPDE Matérn with barriers”). The SPDE Matérn with barriers is often useful in modeling coastal species in areas with complex coastlines (such as the Gulf of Maine) that have islands, bays, peninsulas, or points, because the model’s barriers ensure that correlations between two locations are calculated based on the distance over water between the locations (Bakka et al. 2019). Geospatial data were transformed to the UTM Zone 19 projection (WGS 84 datum), defined by units of kilometers (km) to facilitate model fitting.

Building the spatial component of each DSM required defining a mesh, or triangulated lattice (Lindgren et al. 2011). The mesh is composed of a set of vertices (or "knots") that correspond to each of the spatial random effects. Different meshes could result in different estimates of bird density. There are no strict rules on how to create a mesh for a particular set of observations. We used preliminary analyses with a variety of meshes to guide our decisions on which mesh was best suited to the data. The final parameterization is discussed below. A single mesh was used for all SPDE Matérn DSMs; likewise, a single mesh was used for all DSMs based on the SPDE Matérn with barriers. Initial knot locations were placed at the transect segment midpoints. To eliminate boundary effects, Lindgren and Rue (2015) recommend extending the outer boundary of the

spatial domain that is used for model-building. We refer to the extended domain outside the aerial survey study area as the "buffer area." The extension radius used to set the overall boundary of the spatial domain (hence, the width of the buffer area) was approximately 35% of the diameter of the aerial survey study area. We reduced the knot density in the buffer area to minimize the additional computational burden of the knots located far from survey observations. The maximum distance between knots was 30 km in the study area and 60 km in the buffer area. The minimum distance between knots equaled 1/5 the maximum distance between knots; transect segments located closer than this minimum distance were replaced with a single knot. The mesh for the SPDE Matérn models with barriers assumed that the spatial range over land was 0.1 times that over water.

The full suite of dynamic environmental variables that were considered as potential predictor variables included sea surface salinity, mixed layer thickness, potential temperature, sea surface temperature, magnitude of surface wind velocity, sea level anomaly, chlorophyll *a* concentration, and surface current velocity magnitude. The static environmental variables that were considered as potential predictor variables were seafloor depth, rugosity, sediment class, and distance to shore. Correlation tests (Kendall's Tau and Spearman's Rho) were used to identify potential dynamic and static environmental variables with statistically significant correlations ($p = 0.05$). When significant correlations existed, only one variable was retained for model-building based on ecological understanding of the ecosystem. The five environmental variables retained for model-building were sea surface temperature, current velocity, depth, rugosity, and sediment class.

For each combination of season and taxon, we evaluated purely spatial DSMs and DSMs with both spatial and environmental variables. The DSMs with both spatial and environmental terms included all five environmental variables in the linear predictor. Each environmental variable entered the model as a univariate thin-plate regression spline with shrinkage, allowing the term to shrink to zero during model fitting if the term was not important for describing the spatial pattern of the observations (Wood 2003).

The basic DSM structure for taxon *i* in season *j* at location *k* may be represented as (Bravington et al. 2021):

$$\mathbb{E}\left[\mathrm{Y}_{i,j,k}|\boldsymbol{\beta}_{i,j}\right] = a_{j,k}exp\left[\beta_{i,j,0} + \sum_{q} f_{i,j,q}\left(u_{i,j,k,q}\right)\right] \quad [1]$$

where

$a_{j,k}$ = area corresponding to season *j* and location *k,* which equals the total area within the imagery located in each transect segment for model-building and the cell area for predicting (see abundance estimation methods below);

$Y_{i,j,k}$ = random variable for the number of birds from taxon *i* in season *j* at location *k*;

$u_{i,j,k,q}$ = covariates (indexed by *q*) that influence bird density (in this case, projected latitude and longitude, and possibly the environmental covariates listed above);

$f_{i,j,q}$ = smooth function for the i^{th} species, j^{th} season, and q^{th} covariate;

$\boldsymbol{\beta}_{i,j}$ = vector of parameters in the smooth functions for taxon *i* in season *j*; for simplicity, we include in this vector the intercept parameter $\beta_{i,j,0}$.

As is typical for analyses of digital aerial survey data (e.g., Buckland et al. 2012), we assumed that all birds located at the surface of the water and available to be seen in the imagery were detected. Hence, $Y_{i,j,k}$ is more precisely defined as the number of available birds of taxon *i* in season *j* and location *k*.

We formulated each DSM using a logarithmic link function. We evaluated seven different probability distributions for the likelihood: Tweedie, Poisson, delta gamma, delta lognormal, Poisson delta gamma, Poisson delta lognormal (Thorson 2018), and negative binomial.

Gulf of Maine Surveys: Density Surface Model Evaluation

Each seasonal DSM was evaluated based on the following metrics: conditional AIC (cAIC; Zheng et al. 2024); model evaluation criteria flagged by the sdmTMB *sanity* function (Anderson et al. 2024), including model convergence and relative magnitudes of key parameters; the number of segments with sightings; residual analyses (PIT residuals via R package DHARMa; Hartig 2024); and visual inspections of maps showing model predictions with the sightings overlaid. Models were excluded from further evaluation if they exhibited one or more of the following problems: at least one flag returned by the *sanity* function; ≤ 6 segments with sightings; poor fit to the data based on residual analyses or visual inspection of prediction maps. For each taxon (or buoy) and season, we chose the single best model with the lowest cAIC.

Gulf of Maine Surveys: Availability Bias

Diving birds spend a proportion of their time underwater where they are not visible in imagery from aerial surveys. If an abundance estimate is not corrected for the probability that a bird will be available to be seen during data collection, then the estimate will be subject to availability bias (Marsh & Sinclair 1989). Birds that spend a low proportion of time at the surface where observers can detect them (i.e., low availability) will be detected infrequently relative to their true density (i.e., raw counts will have considerable bias relative to true abundance). Availability probability is the inverse of the availability bias correction factor; it is a function of the bird's respiratory and/or foraging patterns and the duration of time in which the bird is in view. Due to the short period of time in which a particular point on the ocean's surface is in view during digital aerial surveys flown

at 220 km/hr (~120 kts), we used an instantaneous estimate of availability, which is a function of the bird's surface interval (*s*) and dive interval (*d*):

$$\hat{p}_a = \frac{s}{s+d} \quad [2]$$

Availability probability ($\hat{p}_a$) can vary by species, age or life stage, season, location, activity state, and other factors. We estimated availability probability at the species level, $\hat{p}_{a,i}$.

The species that commonly dive and for which there were sufficient sample sizes to build DSMs were the Common Murre (*Uria aalge*), Atlantic Puffin (*Fratercula arctica*), and Dovekie (*Alle alle*). Because there were no estimates of availability specific to the Gulf of Maine for these species, we conducted a literature review and based our estimates of availability probability on the best available information. We estimated availability probability as the fraction of time birds could be observed at the surface or in flight. We did not account for availability probability in the seasonal DSMs for all bird sightings combined because the availability probability of sightings that were not identified to species is unknown.

For Common Murres, Cairns et al. (1987) indicated substantial variability in availability probability based on breeding stage: the availability probability during incubation was approximately 0.80–0.95, and during chick rearing was approximately 0.79–0.86. Burke and Montevecchi (2018) indicated that the availability probability of Common Murres in winter was around 0.89. We set availability probability to 0.80, the approximate midpoint of the reported range in values, although we acknowledge that the true availability probability is context-specific and seasonally variable.

For Atlantic Puffins, we estimated availability probability as the average of Dunn et al.'s (2024) availability probability estimates for the non-breeding period: $\hat{p}_a$ = 0.83.

Availability probability estimates for Dovekies range from approximately 0.77 (Harding et al. 2009) to 0.88 (Karnovsky et al. 2011). Given that the oceanographic conditions in the Gulf of Maine are most similar to the Sørkapp Current, we based our estimate of availability probability on the Hornsund colony data (Karnovsky et al. 2011), $\hat{p}_a$ = 0.797.

Gulf of Maine Surveys: Abundance Estimation

Abundance estimates from each seasonal DSM were based on a hexagonal grid (the prediction surface) with cell centroids located 4 km (2.16 NM) apart. The predicted number of birds in each hexagon in each season, $\hat{Y}_{i,j,k}$, was based on the relationships defined in Eq. [1], where a_k is the total area of the hexagon, which was constant across seasons. For each seasonal DSM, we used the sdmTMB function *simulate.sdmTMB* to simulate 1000 samples of abundance for each cell ($\hat{Y}_{i,j,k}$) by setting the fixed effects to their maximum likelihood estimates, randomly drawing the random effects (independently for each iteration) from a multivariate normal distribution, and excluding observation error. A Horvitz-Thompson estimate was used to predict the number of

birds in the study area in each season for each simulation, based on the sum of cell-specific abundance estimates ($\hat{Y}_{i,j,k}$), divided by the estimated availability probability ($\hat{p}_{a,i}$) from Eq. [2]:

$$\widehat{N}_{i,j} = \frac{\sum_k \hat{Y}_{i,j,k}}{\hat{p}_{a,i}} \quad [3]$$

Then, we computed the abundance estimate for each seasonal DSM as the median value of $\widehat{N}_{i,j}$ among all simulations. The lower and upper 95% confidence intervals on $\widehat{N}_{i,j}$ were computed from the 2.5th and 97.5th quantiles of the simulated distribution of $\widehat{N}_{i,j}$.

Model Comparison: Spatial Cross-correlation

We used spatial cross-correlation (SCC) analysis (Chen 2015) to make two types of comparisons between the MDAT (regional) and BOEM Gulf of Maine (local) models for all 14 species or species groups for which local models could be developed, including Atlantic Puffin, Dovekie, murre spp. (almost entirely made up of Common Murres), Black-Legged Kittiwake (*Rissa tridactyla*), Bonaparte's Gull (*Chroicocephalus philadelphia*), Laughing Gull (*Leucophaeus atricilla*), Ring-billed Gull (*Larus delawarensis*), American Herring Gull (*L. smithsonianus*), Great Black-backed Gull (*L. marinus*), Common Tern (*Sterna hirundo*), tern spp. (*Sterna* spp.), Wilson's Storm-Petrel (*Oceanites oceanicus*), Northern Fulmar (*Fulmarus glacialis*), and Northern Gannet (*Morus bassanus*). The first comparison examined the relationships between the scaled estimates of the relative density (regional) and absolute abundance (local) of birds by season, using the monthly estimates from the regional models to compare to the same months in the local models. Twenty-four taxon-season pairs were modeled at the local scale and examined in the SCC analysis. The second comparison was between the scaled estimates of the respective coefficients of variation (CVs) for these same models. The comparison of CVs was supplemental, to explore potential reasons for differences in the spatial patterns between the regional and local models. To compute the SCC statistics and produce the figures, we used a combination of customized code based on Chen's (2015) methods and the *crossCorrelation* function from the *spatialEco* package (Evans and Murphy 2023).

Estimates of local abundance for the SCC analysis were derived by projecting the local models onto the n = 70 centroids of the raster cells from the regional model predictions that were located within the Gulf of Maine study area. The local CV estimates were generated for the same cell centroids using the methods described above to estimate the CV for each cell in the original Gulf of Maine hexagonal prediction grid.

Local DSMs were created for murre spp. and tern spp. To produce analogous relative density estimates for these groups from the regional prediction rasters, we computed cellwise sums of Common Murre and Thick-billed Murre (*Uria lomvia*) densities to represent the murre spp. group, and we summed cellwise estimates of Arctic Terns (*Sterna paradisaea*), Common Terns, Forster's

Terns (*S. forsteri*), and Roseate Terns (*S. dougallii*) to represent the tern spp. group. Although availability and detection bias were not accounted for in the regional models, we felt it was reasonable to sum the model predictions across species within these species groups, assuming that these biases would be relatively similar for related species. We did not estimate the CVs of the density estimates from the regional models for these pooled species groups.

We used Chen's (2015) methods to scale the cellwise values of the estimated parameters (density or abundance, and CV) for each taxon. Scaling was done independently for each combination of taxon (i.e., species or species group, indexed by *i*), season (*j*), and model (i.e., regional or local, indexed by *m*). The scaling process required computing standard scores based on the mean and population variance of the estimated parameters for locations in the Gulf of Maine study area. The mean was computed as:

$$\hat{\mu}_{x,i,j,m} = \frac{1}{n_c}\sum_{c=1}^{n_c} \hat{x}_{i,j,c,m}$$

where,

c = index for hex cell location, *c* = 1,..., n_c;

n_c = number of hex cell centroids in the study area, n_c=70;

$\hat{x}_{i,j,c,m}$ = estimated value of parameter *x* (i.e., density, abundance, or CV) from model *m* for taxon *i* in season *j* at location *c*; and

$\hat{\mu}_{x,i,j,m}$ = estimated mean value of parameter *x* in the study area from model *m* for taxon *i* in season *j*.

The estimated population variance of parameter *x* in the study area is computed as:

$$\hat{\sigma}^2_{x,i,j,m} = \frac{1}{n_c}\sum_{c=1}^{n_c}\left(\hat{x}_{i,j,c,m} - \hat{\mu}_{x,i,j,m}\right)^2$$

Finally, the scaled estimate of parameter *x* from model *m* for taxon *i* in season *j* at location *c* was:

$$\tilde{x}_{i,j,c,m} = \frac{\hat{x}_{i,j,c,m} - \hat{\mu}_{x,i,j,m}}{\hat{\sigma}_{x,i,j,m}}$$

SCC compares the spatial pattern of the values from two measures (e.g., variables, parameters, indices, etc.). The local spatial cross-correlation index (LSCI) quantifies the cross-correlation between the value from one measure at a given location and the values from the other measure at all other locations in a geographical system. Our SCC analysis that treated local abundances as the independent variable and regional densities as the dependent variable produced 70 LSCI indices; each one represented the cross-correlation between the scaled value from the local

model at one centroid and the scaled values from the regional model at all other centroids in the study area. Analogously, the SCC analysis that treated the regional densities as the independent variable and the local abundances as the dependent variable also produced 70 LSCI indices, with each LSCI representing the cross-correlation between the scaled value from the regional model at one centroid and the scaled values from the local model at all other centroids in the study area.

The weights given to the values of neighboring cells in the LSCI computation were a function of the distance between centroids. The effect of distance on the weights was defined by either an inverse distance relationship or a negative exponential relationship. Inverse distance weighting allowed the analysis to give relatively more weight to distant neighbors than the negative exponential weighting does.

The global spatial cross-correlation index (GSCI) is a single value that is computed as the sum of the LSCIs. The GSCI explains the broadscale spatial cross-correlation between the two measures across the entire study area. GSCI values range between -1.0 and 1.0. The larger the absolute value of the GSCI, the stronger the correlation. Positive GSCI values indicate that areas of high scaled values in one measure generally align with areas of high scaled values in the second measure, and lows align with lows (i.e., positive correlation). In contrast, negative GSCI values indicate that there is a mismatch in the areas with low and high scaled values between the measures (i.e., negative correlation). Goodness-of-fit in the relationship between the LSCIs and the GSCI is estimated separately through the coefficient of determination statistic R^2. While we were not trying to determine if the avian density patterns from the regional models were shaping the density patterns from the local models (or vice versa), R^2 indicated how complementary the two models were in their predictions.

Model Comparison: Center of Gravity

Because the spatial extent of the regional models was larger than the local models, and the resolution of the regional analysis was coarser than that of the local models, we computed the center of gravity (COG) statistic from Thorson et al. (2016). This statistic provides a simple way to show the center of a species predicted distribution on a map, and it can account for spatially variable survey effort. The COG weighted spatial coordinates of the centroid of each cell by the estimated abundance or relative density of birds at each location:

$$C_x = \frac{\sum_{c=1}^{n_c} \widehat{N}_c x_c}{\sum_{c=1}^{n_c} \widehat{N}_c}$$

$$C_y = \frac{\sum_{c=1}^{n_c} \widehat{N}_c y_c}{\sum_{c=1}^{n_c} \widehat{N}_c}$$

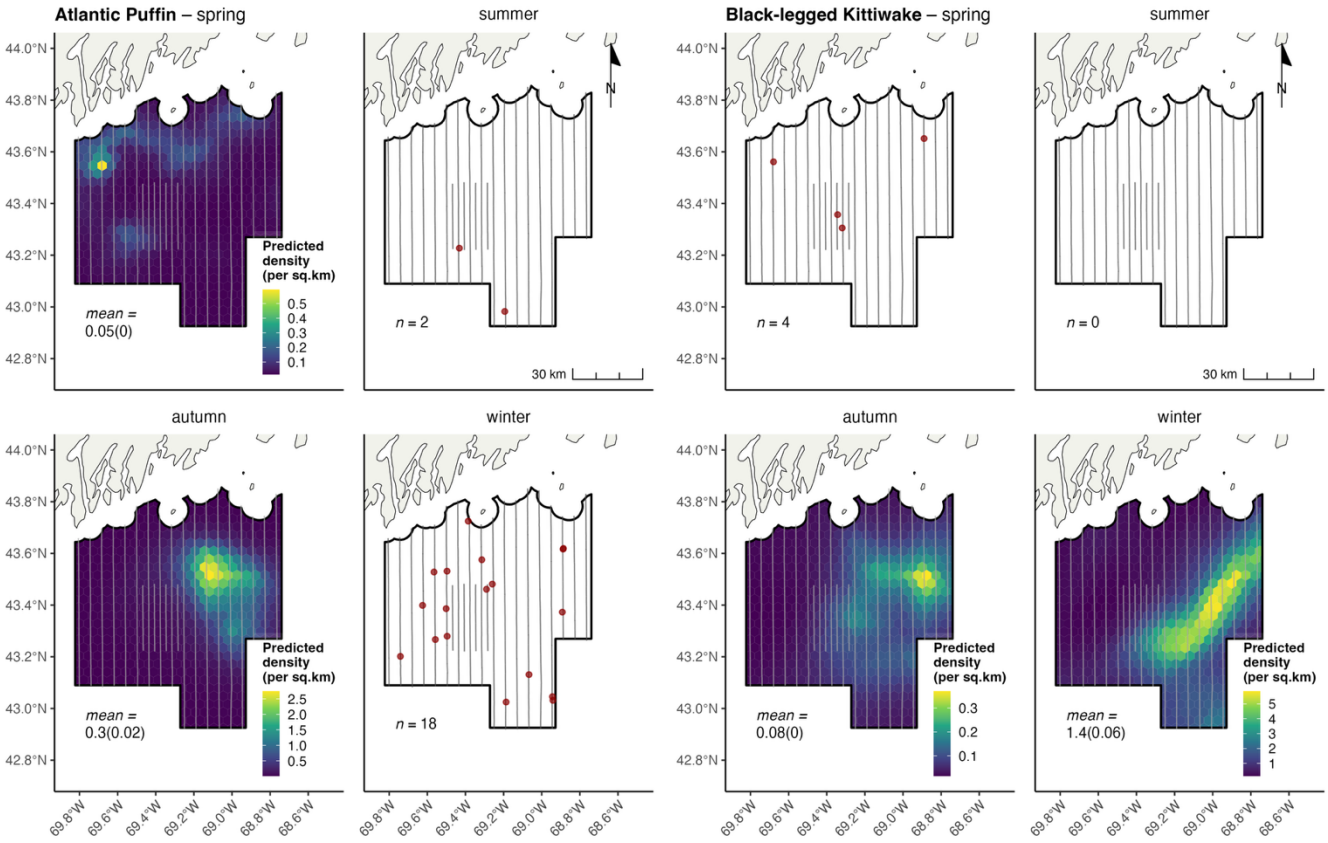
where C_x is the COG for the x-coordinate, $C_y$is the COG for the y-coordinate, $\widehat{N}_c$ is the estimated abundance (local model) or relative density (regional model) at centroid c, and the denominator equals the total estimated abundance or relative abundance in the study area. We based the COG analysis on the raw model output, i.e., the relative density estimates from the regional models and absolute abundance estimates from the local models.

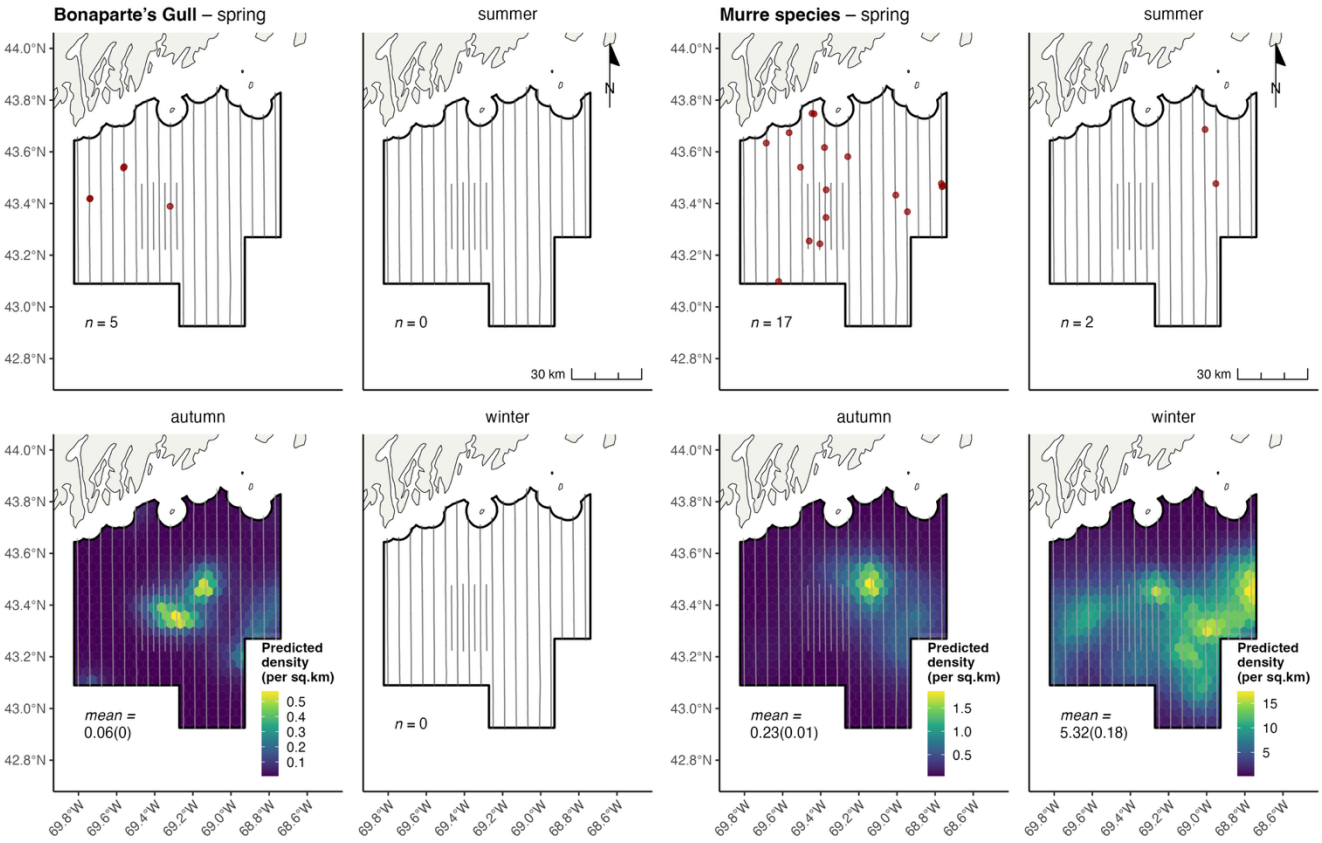
SUPPLEMENTARY FIGURES AND TABLES

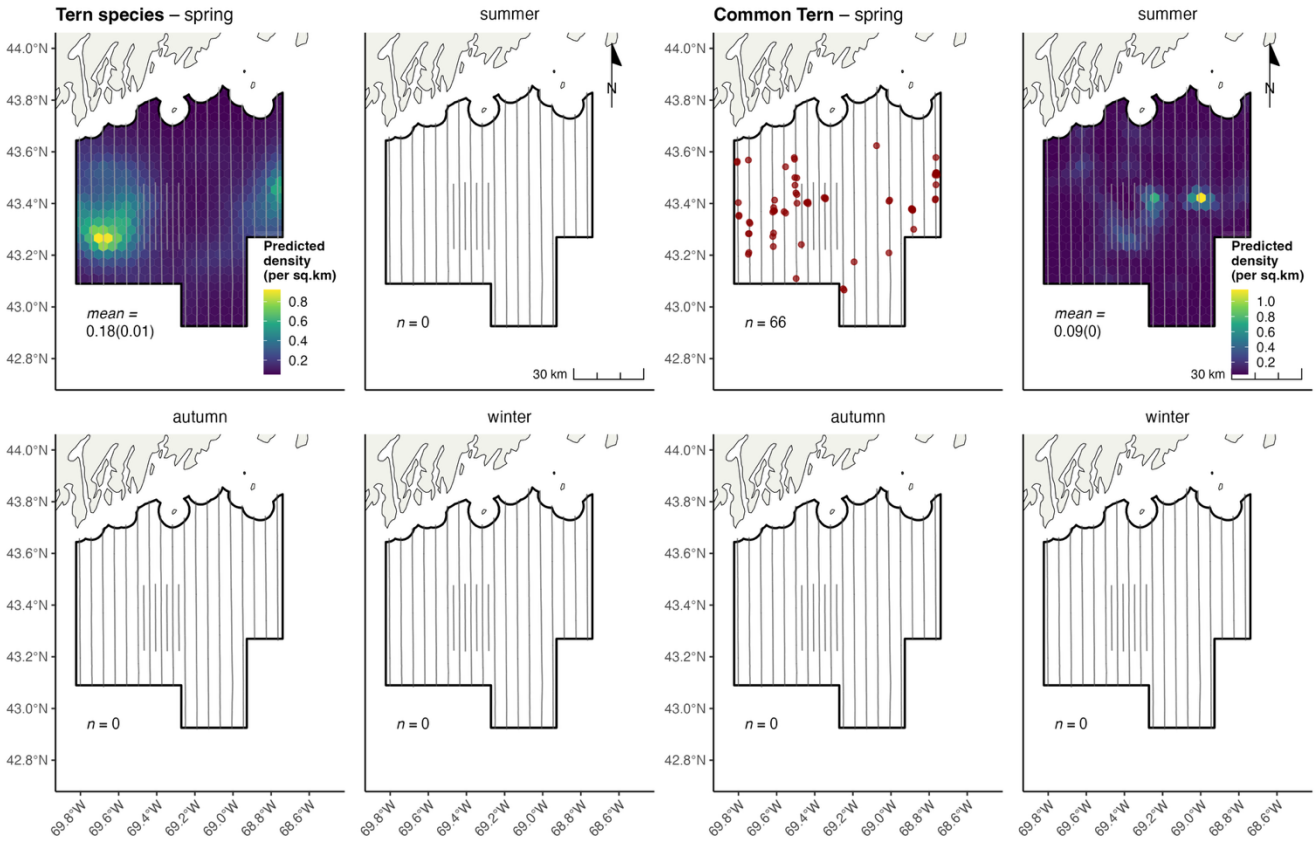
Table A1. Data products used for dynamic and static environmental covariates in the local density surface models for the Gulf of Maine study area.

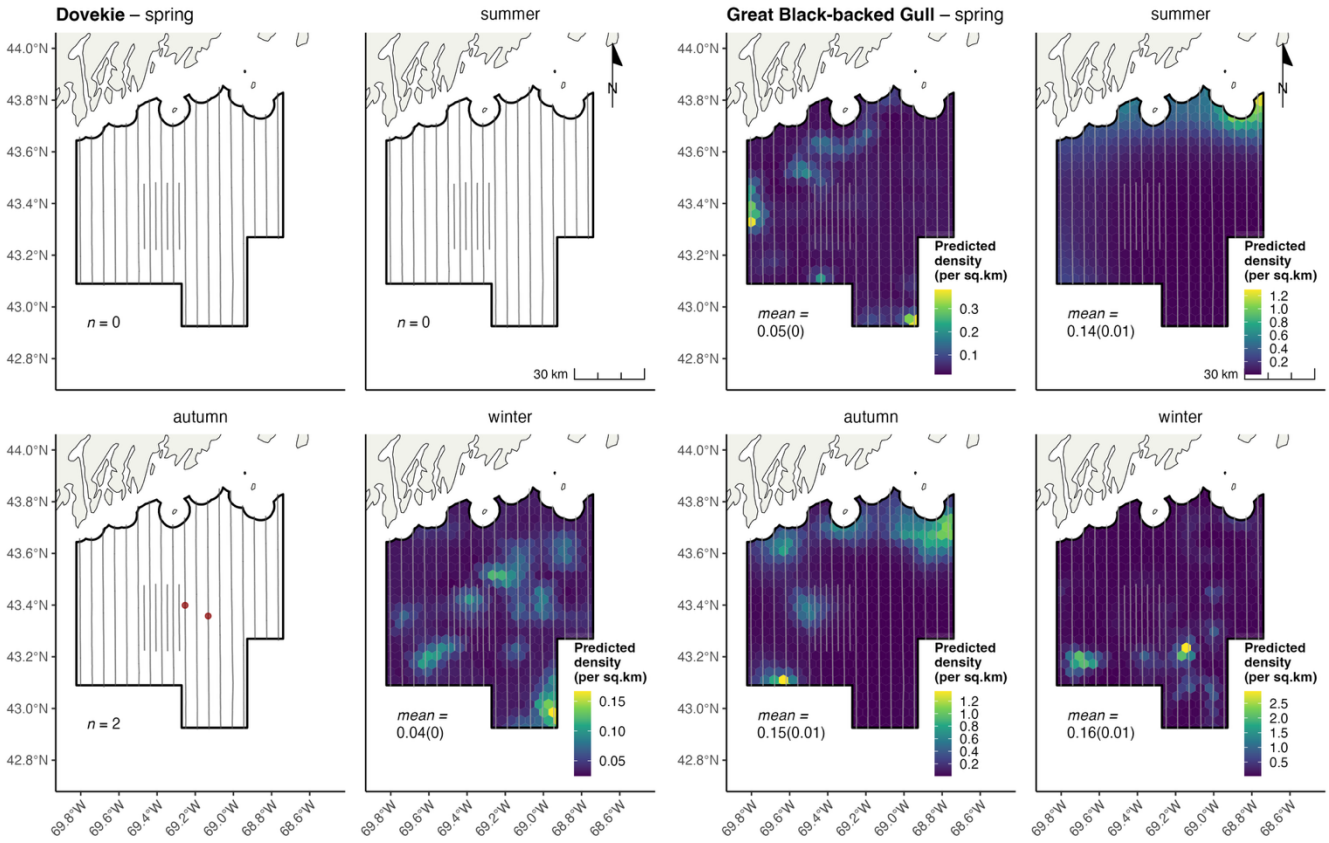
	Predictor	Description	Temporal	Spatial	Units	Source	URL
Dynamic	salinity	Mean of daily sea surface salinity (depth = 0)	Monthly	8 km	psu	Global Ocean Physics Reanalysis (GLORYS 12V1)	https://doi.org/10.48670/moi-00021
	mixed layer thickness	Mean of daily depth where the density increase compared to density at 10 m depth corresponds to a temperature decrease of 0.2°C in local surface conditions (θ10 m, S10 m, P0 = 0 db, surface pressure)	Monthly	8 km	m	GLORYS12V1	https://doi.org/10.48670/moi-00021
	potential temperature	Mean of daily temperature a parcel of seawater if moved without heat exchange to the sea surface (depth = 0)	Monthly	8 km	°C	GLORYS12V1	https://doi.org/10.48670/moi-00021
	sea surface temperature	Mean of daily sea surface temperature	Monthly	1 km	°C	NASA PODAAC Multiscale Ultrahigh Resolution (MUR) Sea Surface Temperature	https://eastcoast.coastwatch.noaa.gov/data/podaac-mur/sst/monthly/conus/
	surface wind velocity magnitude	Scalar average 10-m wind speed	Monthly	28 km	m/s	Mears, C.; Lee, T.; Ricciardulli, L.; Wang, X.; Wentz, F., 2022: RSS Cross-Calibrated Multi-Platform (CCMP) monthly ocean vector wind analysis on 0.25 deg grid, Version 3.0, Remote Sensing Systems, Santa Rosa, CA. Available at www.remss.com	https://doi.org/10.56236/RSS-uv1m30
	sea level anomaly	Altimeter satellite gridded anomalies computed with	Monthly	14 km	m	Global Ocean Gridded L 4 Sea Surface Heights and Derived Variables Reprocessed 1993 Ongoing	https://doi.org/10.48670/moi-00148

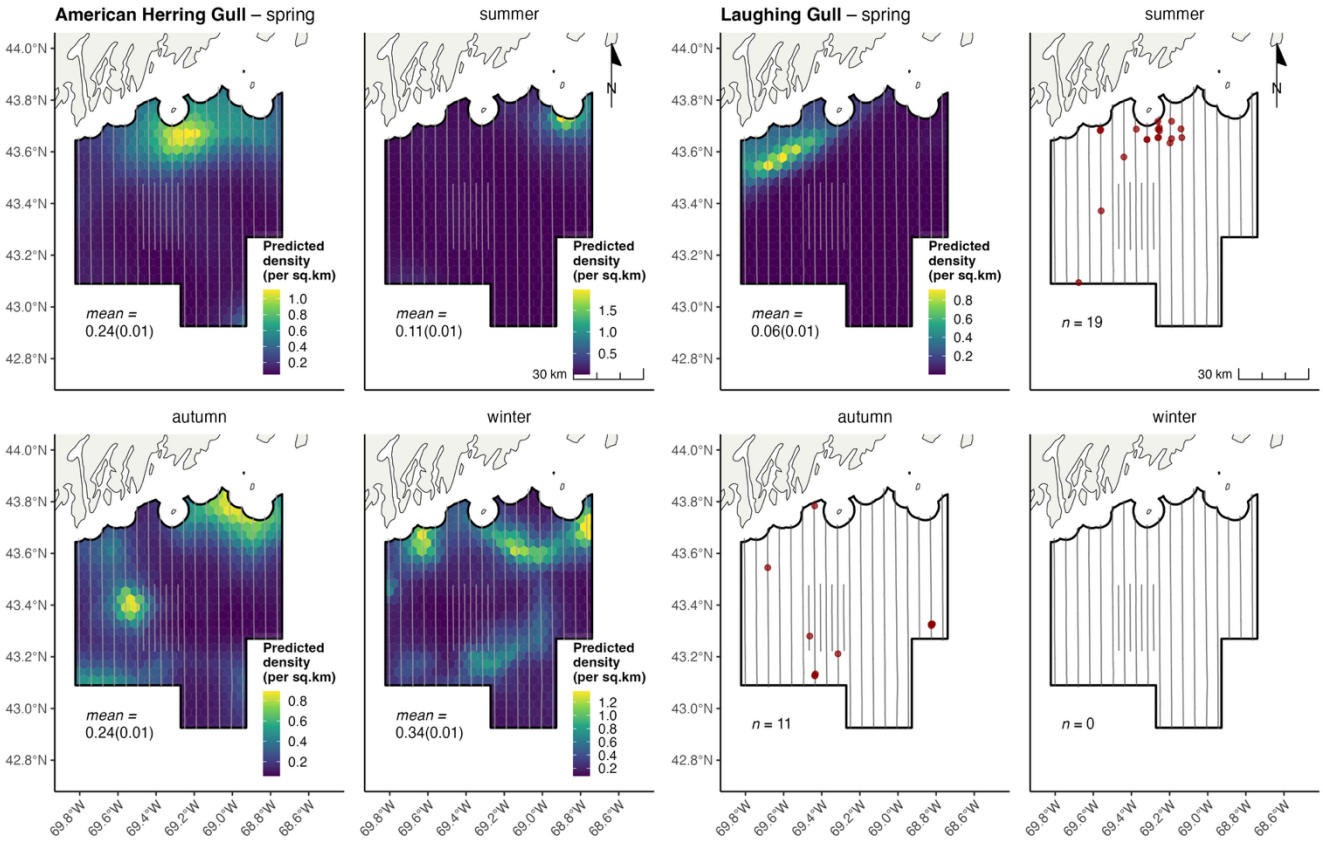
	Predictor	Description	Temporal	Spatial	Units	Source	URL
		respect to a twenty-year mean (1993–2012)					
	chlorophyll *a*	Mean of daily mass concentration of chlorophyll *a* in seawater (depth = 0)	Monthly	4 km	mg/m^-3	Global Ocean Colour (Copernicus-GlobColour), Bio-Geo-Chemical, L4 (monthly and interpolated) from Satellite Observations (1997-ongoing)	https://doi.org/10.48670/moi-00281
	surface current velocity magnitude	Mean of daily current velocity calculated with northward and eastward components (depth = 0)	Monthly	8 km	m/s	GLORYS12V1	https://doi.org/10.48670/moi-00021
Static	depth	Measured and estimated seafloor bathymetry		1 km	m	GEBCO Compilation Group (2024) GEBCO 2024 Grid	https://www.gebco.net/data-products-gridded-bathymetry-data/gebco2024-grid
	rugosity	Measure of small-scale variations of amplitude in the height of a surface / seafloor complexity		0.5 km	ratio of real to geometric surface area	Friedland, K. D., Langan, J. A., Large, S. I., Selden, R. L., Link, J. S., Watson, R. A., & Collie, J. S. (2020). Changes in higher trophic level productivity, diversity and niche space in a rapidly warming continental shelf ecosystem. Science of the Total Environment, 704, 135270.	https://doi.org/10.1016/j.scitotenv.2019.135270
	sediment class	Interpolated and reclassified percentages of sand, mud, and gravel in marine sediment point-based samples		0.5 km	categorical class	Anderson, M. G., Greene, J., Morse, D., Shumway, D. and Clark, M (2010) Benthic Habitats of the Northwest Atlantic in Greene, J.K., M.G. Anderson, J. Odell, and N. Steinberg, eds. The Northwest Atlantic Marine Ecoregional Assessment: Species, Habitats and Ecosystems. Phase One. The Nature Conservancy, Eastern U.S. Division, Boston, MA.	https://portal.midatlanticocean.org/static/data_manager/metadata/html/SoftSediment_2020_metadata.html
	distance to shore	Shortest distance to the continental United States		4	km	Derived from: Wessel, P., and W. H. F. Smith. (1996) A Global Self-consistent, Hierarchical, High-resolution Shoreline Database. Journal of Geophysical Research 101: 8741-8743.	https://www.soest.hawaii.edu/pwessel/gshhg/

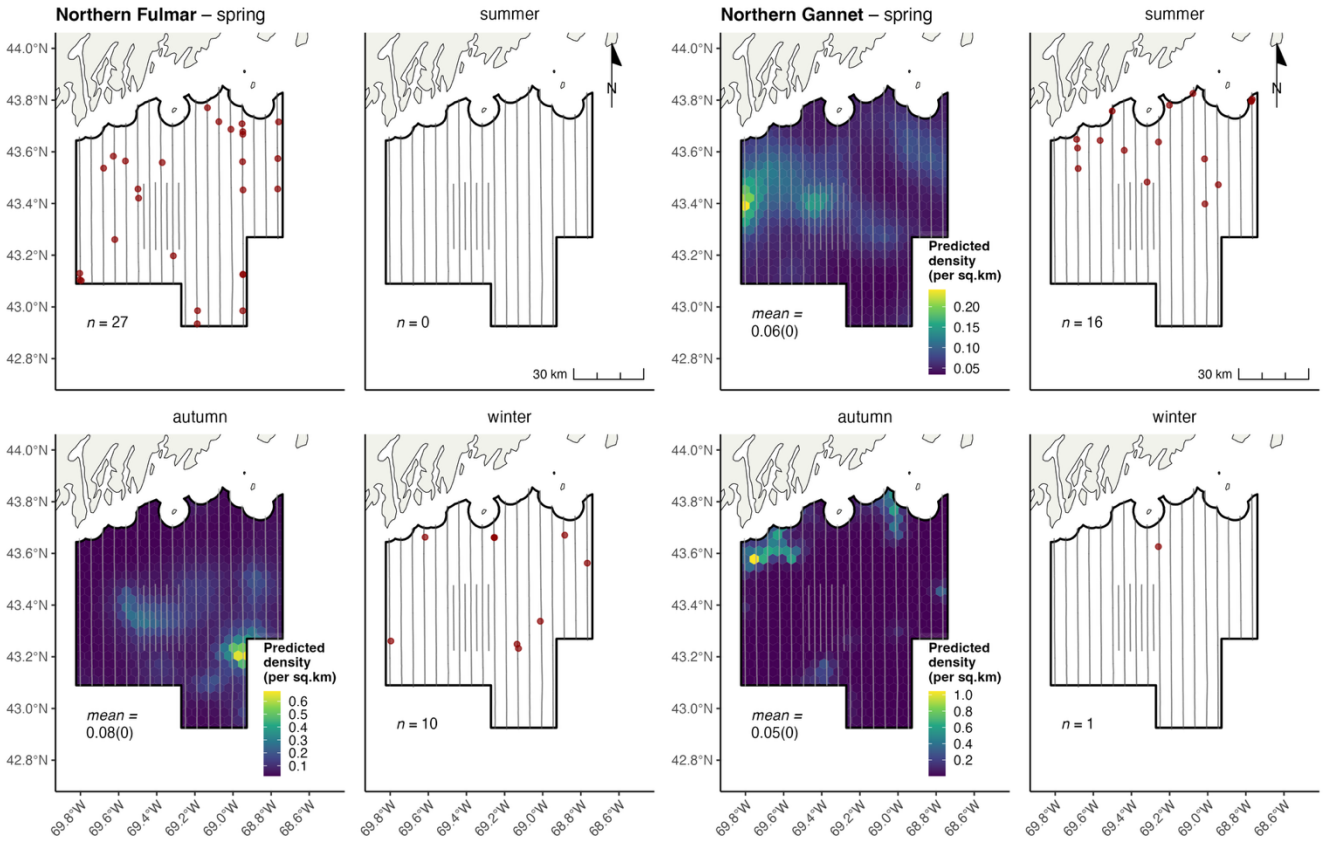

Atlantic Puffin – spring
summer
Black-legged Kittiwake – spring
summer
autumn
winter
autumn
winter
Predicted density (per sq.km)
mean = 0.05(0)
n = 2
n = 4
n = 0
mean = 0.3(0.02)
n = 18
mean = 0.08(0)
mean = 1.4(0.06)
30 km
N
44.0°N
43.8°N
43.6°N
43.4°N
43.2°N
43.0°N
42.8°N
69.8°W
69.6°W
69.4°W
69.2°W
69.0°W
68.8°W
68.6°W


Bonaparte's Gull – spring
summer
Murre species – spring
summer
autumn
winter
autumn
winter
n = 5
n = 0
n = 17
n = 2
30 km
N
mean = 0.06(0)
mean = 0.23(0.01)
mean = 5.32(0.18)
Predicted density (per sq.km)
0.5
0.4
0.3
0.2
0.1
1.5
1.0
0.5
15
10
5
44.0°N
43.8°N
43.6°N
43.4°N
43.2°N
43.0°N
42.8°N
69.8°W
69.6°W
69.4°W
69.2°W
69.0°W
68.8°W
68.6°W


Tern species – spring
summer
Common Tern – spring
summer
autumn
winter
autumn
winter
Predicted density (per sq.km)
mean = 0.18(0.01)
n = 0
n = 66
mean = 0.09(0)
30 km
N
44.0°N
43.8°N
43.6°N
43.4°N
43.2°N
43.0°N
42.8°N
69.8°W
69.6°W
69.4°W
69.2°W
69.0°W
68.8°W
68.6°W


Dovekie – spring
summer
Great Black-backed Gull – spring
summer
autumn
winter
autumn
winter
n = 0
n = 0
mean = 0.05(0)
mean = 0.14(0.01)
n = 2
mean = 0.04(0)
mean = 0.15(0.01)
mean = 0.16(0.01)
Predicted density (per sq.km)
30 km
N
44.0°N
43.8°N
43.6°N
43.4°N
43.2°N
43.0°N
42.8°N
69.8°W
69.6°W
69.4°W
69.2°W
69.0°W
68.8°W
68.6°W


American Herring Gull – spring
summer
Laughing Gull – spring
summer
autumn
winter
autumn
winter
Predicted density (per sq.km)
mean = 0.24(0.01)
mean = 0.11(0.01)
mean = 0.06(0.01)
n = 19
mean = 0.24(0.01)
mean = 0.34(0.01)
n = 11
n = 0
30 km
N
44.0°N
43.8°N
43.6°N
43.4°N
43.2°N
43.0°N
42.8°N
69.8°W
69.6°W
69.4°W
69.2°W
69.0°W
68.8°W
68.6°W


Northern Fulmar – spring
summer
Northern Gannet – spring
summer
autumn
winter
autumn
winter
n = 27
n = 0
n = 16
n = 10
n = 1
mean = 0.06(0)
mean = 0.08(0)
mean = 0.05(0)
Predicted density (per sq.km)
0.20
0.15
0.10
0.05
0.6
0.5
0.4
0.3
0.2
0.1
1.0
0.8
0.6
0.4
0.2
30 km
N
44.0°N
43.8°N
43.6°N
43.4°N
43.2°N
43.0°N
42.8°N
69.8°W
69.6°W
69.4°W
69.2°W
69.0°W
68.8°W
68.6°W

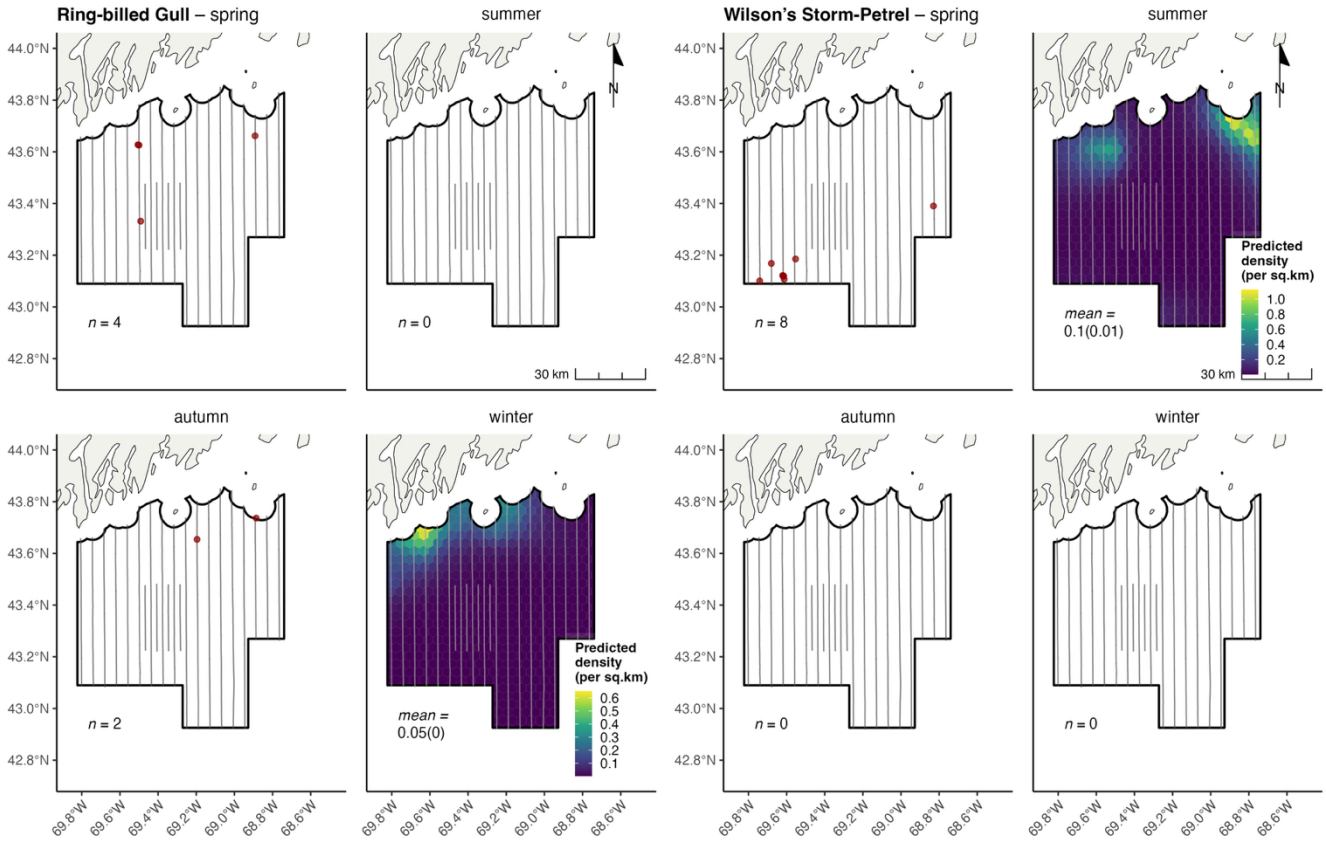


Figure A1. Median number of birds per km^2 predicted from local density surface models and corrected for availability. Density value scales are specific to each season and taxon, and predicted values are all greater than zero. Raw sightings of individuals (points) are provided when seasonal density models were not possible. Text annotations in bottom left show total sightings (*n* =) or mean seasonal bird densities per km^2 and standard error for the 2023–2024 Gulf of Maine survey area.

Table A2. Seasonal density surface models selected for each avian species/group and all birds for the 2023-24 Gulf of Maine survey area. All best models used spatial random effects defined by a stochastic partial differential equation approximation to model the precision matrix associated with the Matérn covariance function accounting for coastline barriers.

Species or group	Season	Observation likelihood	No. of random effects	Effective degrees of freedom	No. of segments with sightings	Total No. of sightings	Availability probability	2.5th quantile on abundance estimate	Median abundance estimate	97.5th quantile on abundance estimate	Standard error of abundance estimate
Atlantic Puffin	spring	Poisson	185	20.8	26	36	0.83	344	476	651	79
	autumn	Negative Binomial	199	20.2	69	201	0.8	1763	2413	3298	394
Black-legged Kittiwake	autumn	Tweedie	199	13.6	38	64	1	474	636	856	102
	winter	Negative Binomial	197	24.7	211	1170	1	8602	10234	12071	909
Bonaparte's Gull	autumn	Negative Binomial	199	19.9	28	93	1	402	654	1125	191
Common Murre / murre spp	autumn	Tweedie	199	19.2	68	148	0.8	1428	1793	2267	214
	winter	Tweedie	197	49.2	314	3315	0.8	35779	38028	40707	1294
Common Tern / tern spp	spring	Poisson Delta Gamma	370	19.7	47	143	1	1093	1441	1998	232
Common Tern	summer	Tweedie	194	25.7	49	95	1	684	841	1034	90
Dovekie	winter	Poisson Delta Gamma	394	28.1	27	32	0.797	300	372	465	42
Great Black-backed Gull	spring	Poisson Delta Gamma	370	42.7	30	45	1	338	429	585	66
	summer	Negative Binomial	194	14	50	95	1	676	896	1230	148
	autumn	Tweedie	199	30.3	47	122	1	895	1220	1624	194
	winter	Tweedie	197	49.4	65	159	1	1184	1446	1810	160
American Herring Gull	spring	Negative Binomial	185	15.7	78	200	1	1330	1794	2459	283
	summer	Negative Binomial	194	18.6	45	92	1	558	767	1055	135
	autumn	Negative Binomial	199	22.9	89	211	1	1425	1787	2297	221
	winter	Negative Binomial	197	27.1	100	328	1	2201	2752	3546	347

Species or group	Season	Observation likelihood	No. of random effects	Effective degrees of freedom	No. of segments with sightings	Total No. of sightings	Availability probability	2.5th quantile on abundance estimate	Median abundance estimate	97.5th quantile on abundance estimate	Standard error of abundance estimate
Laughing Gull	spring	Negative Binomial	185	15.7	78	200	1	1330	1794	2459	283
Northern Fulmar	autumn	Negative Binomial	199	23.1	49	78	1	502	672	902	103
Northern Gannet	spring	Negative Binomial	185	10.4	37	58	1	395	507	679	72
	autumn	Poisson	199	34.1	26	43	1	335	485	725	122
Ring-billed Gull	winter	Negative Binomial	197	11.4	21	37	1	228	378	637	105
Wilson's Storm-Petrel	summer	Negative Binomial	194	14	23	132	1	547	1045	2261	482
All birds	spring	Negative Binomial	185	16.7	191	676	1	5238	6126	7225	522
	summer	Poisson Delta Lognormal	388	24.9	157	591	1	4155	4881	5601	375
	autumn	Negative Binomial	199	40.4	253	1180	1	8741	9974	11361	689
	winter	Poisson Delta Lognormal	394	48.1	354	5212	1	46698	50771	55472	2277

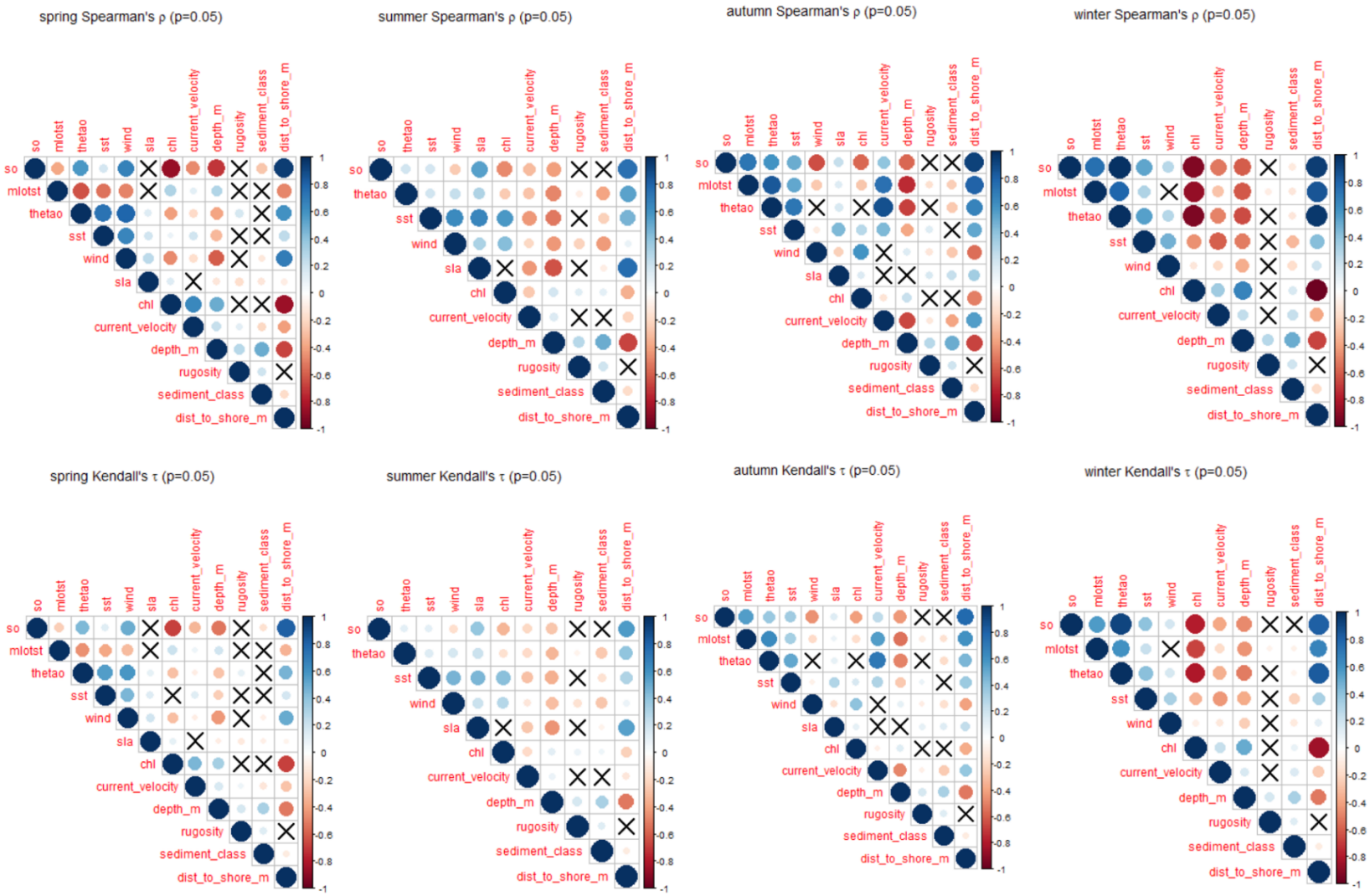


Figure A2. Spearman's rho (top) and Kendall's tau (bottom) correlation tests for environmental predictors in local surface density models by season. Dynamic predictors included salinity (so), mixed layer thickness (mlotst), potential temperature (thetao), sea surface temperature

(sst), surface wind velocity magnitude (wind), sea level anomaly (sla), chlorophyll a (chl), surface current velocity magnitude (current velocity), and static predictors included water depth, rugosity, sediment class, and distance to shore (m).

Table A3. Availability correction factors ($\hat{p}_a$) for three diving marine bird species used in local density surface models for the 2023-24 Gulf of Maine survey area. Correction factors are defined as the proportion of time an individual is visible at the ocean surface (possible range: 0-1).

Species	$\hat{p}_a$	References
Atlantic Puffin - spring	0.83	Dunn et al. 2024
Atlantic Puffin - autumn	0.8	Spencer 2012
Common Murre	0.8	Cairns et al. 1987, Burke & Montevecchi 2018
Dovekie	0.797	Karnovsky et al. 2011

Table A4. All bird sightings by season from 2023–24 digital aerial surveys in the Gulf of Maine survey area. Asterisks (*) indicate species included in local density surface models.

Species	May 2023	August 2023	October 2023	January 2024	TOTAL
American Herring Gull*	200	92	211	328	**831**
Arctic Tern*	2	5	0	0	**7**
Atlantic Puffin*	36	2	201	18	**257**
Black-legged Kittiwake*	4	0	64	1170	**1238**
Black Scoter	0	0	24	0	**24**
Black Tern*	0	4	0	0	**4**
Bonaparte's Gull*	5	0	93	0	**98**
Common Eider	0	0	66	0	**66**
Common Loon	6	0	18	0	**24**
Common Murre*	17	2	146	3312	**3477**
Common Tern*	66	95	0	0	**161**
Double-crested Cormorant	3	1	0	0	**4**
Dovekie*	0	0	2	32	**34**
Great Black-backed Gull*	45	95	122	159	**421**
Great Shearwater	1	11	2	0	**14**
Greater Yellowlegs	0	6	0	0	**6**
Iceland Gull	0	0	1	1	**2**
Laughing Gull*	52	19	11	0	**82**
Leach's Storm-Petrel	1	2	0	0	**3**
Lesser Black-backed Gull	0	1	0	0	**1**
Long-tailed Duck	0	0	0	2	**2**
Manx Shearwater	0	1	0	0	**1**
Northern Fulmar*	27	0	78	10	**115**
Northern Gannet*	58	16	43	1	**118**
Osprey	1	0	0	0	**1**
Parasitic Jaeger	0	0	2	0	**2**
Pomarine Jaeger	0	0	4	0	**4**
Razorbill	0	1	22	6	**29**
Red-throated Loon	8	0	1	2	**11**
Ring-billed Gull*	4	0	2	37	**43**
Surf Scoter	0	0	25	0	**25**
Wilson's Storm-Petrel*	8	132	0	0	**140**
Yellow-bellied Sapsucker	1	0	0	0	**1**
Unidentified large gull	1	1	0	3	**5**
Unidentified loon	0	0	0	1	**1**
Unidentified murre*	0	0	2	3	**5**
Unidentified passerine	3	0	0	0	**3**
Unidentified small gull	1	0	0	0	**1**
Unidentified storm-petrel	1	47	0	0	**48**
Unidentified bird	125	58	40	127	**350**
TOTAL BIRDS	**676**	**591**	**1180**	**5212**	**7659**

Table A5. Global spatial cross-correlation indices (GSCI) of scaled local and regional density estimates and of their respective coefficients of variation (CV) estimates for all taxon/season combinations (*n* = 24). Index values can range from -1 to 1. Coefficients of determination (R^2) indicate goodness-of-fit in the relationship between local spatial cross-correlation indices and the GSCI for the analysis in which the local scaled predictions are treated as the independent (x = local) or dependent (x = regional) variable. CVs for pooled taxa groups were not compared (see Methods). Results from both weighting methods are provided.

		Density						CV(Density)					
		GSCI		R^2 (x=local)		R^2 (x=regional)		GSCI		R^2 (x=local)		R^2 (x=regional)	
Species	**Season**	*Inverse Distance*	*Negative Exponential*	*Inverse Distance*	*Negative Exponential*	*Inverse Distance*	*Negative Exponential*	*Inverse Distance*	*Negative Exponential*	*Inverse Distance*	*Negative Exponential*	*Inverse Distance*	*Negative Exponential*
Atlantic Puffin	spring	0.166	0.224	0.412	0.404	0.734	0.720	-0.104	-0.142	0.185	0.181	0.185	0.181
	autumn	-0.001	0.000	0.000	0.000	0.000	0.000	0.000	0.006	0.000	0.001	0.000	0.001
Black-legged Kittiwake	autumn	0.128	0.177	0.193	0.196	0.240	0.248	0.045	0.063	0.252	0.283	0.036	0.038
	winter	0.146	0.201	0.341	0.343	0.351	0.362	0.036	0.052	0.030	0.033	0.038	0.043
Bonaparte's Gull	autumn	-0.046	-0.057	0.041	0.033	0.091	0.084	-0.021	-0.024	0.009	0.006	0.015	0.010
Common Murre / murre spp	autumn	-0.027	-0.033	0.022	0.018	0.017	0.015	--	--	--	--	--	--
	winter	-0.152	-0.205	0.386	0.373	0.500	0.512	--	--	--	--	--	--
Common Tern / tern spp	spring	0.142	0.199	0.259	0.260	0.493	0.560	--	--	--	--	--	--
Common Tern	summer	0.012	0.015	0.005	0.004	0.011	0.010	0.098	0.128	0.287	0.271	0.322	0.309
Dovekie	winter	-0.046	-0.056	0.044	0.035	0.374	0.389	-0.066	-0.087	0.074	0.067	0.352	0.363
Great Black-backed Gull	spring	0.060	0.083	0.054	0.055	0.322	0.367	0.035	0.051	0.027	0.031	0.047	0.055
	summer	0.112	0.154	0.193	0.194	0.322	0.313	-0.048	-0.069	0.110	0.122	0.040	0.043
	autumn	0.103	0.139	0.197	0.193	0.351	0.344	-0.124	-0.179	0.287	0.318	0.303	0.338
	winter	-0.007	-0.010	0.002	0.002	0.006	0.007	-0.021	-0.026	0.006	0.005	0.046	0.046
American Herring Gull	spring	0.166	0.227	0.585	0.578	0.423	0.430	-0.003	-0.004	0.001	0.001	0.000	0.000
	summer	0.104	0.144	0.210	0.209	0.320	0.323	-0.028	-0.042	0.043	0.053	0.025	0.033
	autumn	0.083	0.111	0.176	0.166	0.272	0.274	-0.018	-0.025	0.010	0.011	0.018	0.021
	winter	0.087	0.114	0.188	0.175	0.366	0.351	-0.003	-0.002	0.000	0.000	0.001	0.000
Laughing Gull	spring	0.120	0.157	0.411	0.367	0.369	0.356	-0.063	-0.089	0.099	0.105	0.115	0.121
Northern Fulmar	autumn	0.034	0.044	0.058	0.060	0.040	0.037	0.111	0.155	0.196	0.200	0.292	0.307
Northern Gannet	spring	0.082	0.118	0.142	0.155	0.164	0.184	0.073	0.105	0.115	0.128	0.123	0.137
	autumn	0.096	0.122	0.193	0.164	0.650	0.593	-0.009	-0.015	0.003	0.004	0.010	0.015
Ring-billed Gull	winter	-0.074	-0.113	0.115	0.147	0.147	0.185	0.080	0.114	0.113	0.121	0.228	0.239
Wilson's Storm-Petrel	summer	-0.094	-0.128	0.291	0.287	0.290	0.299	-0.049	-0.064	0.041	0.037	0.229	0.242

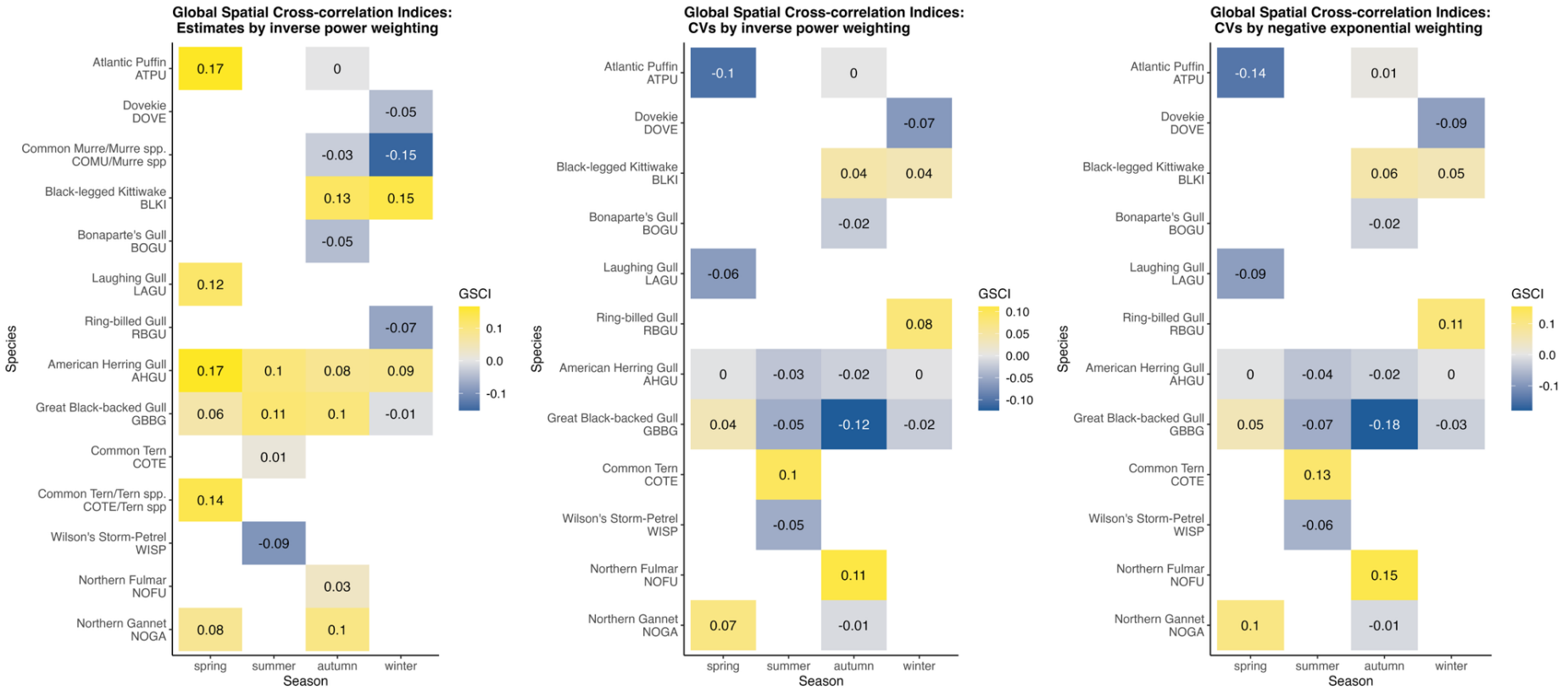
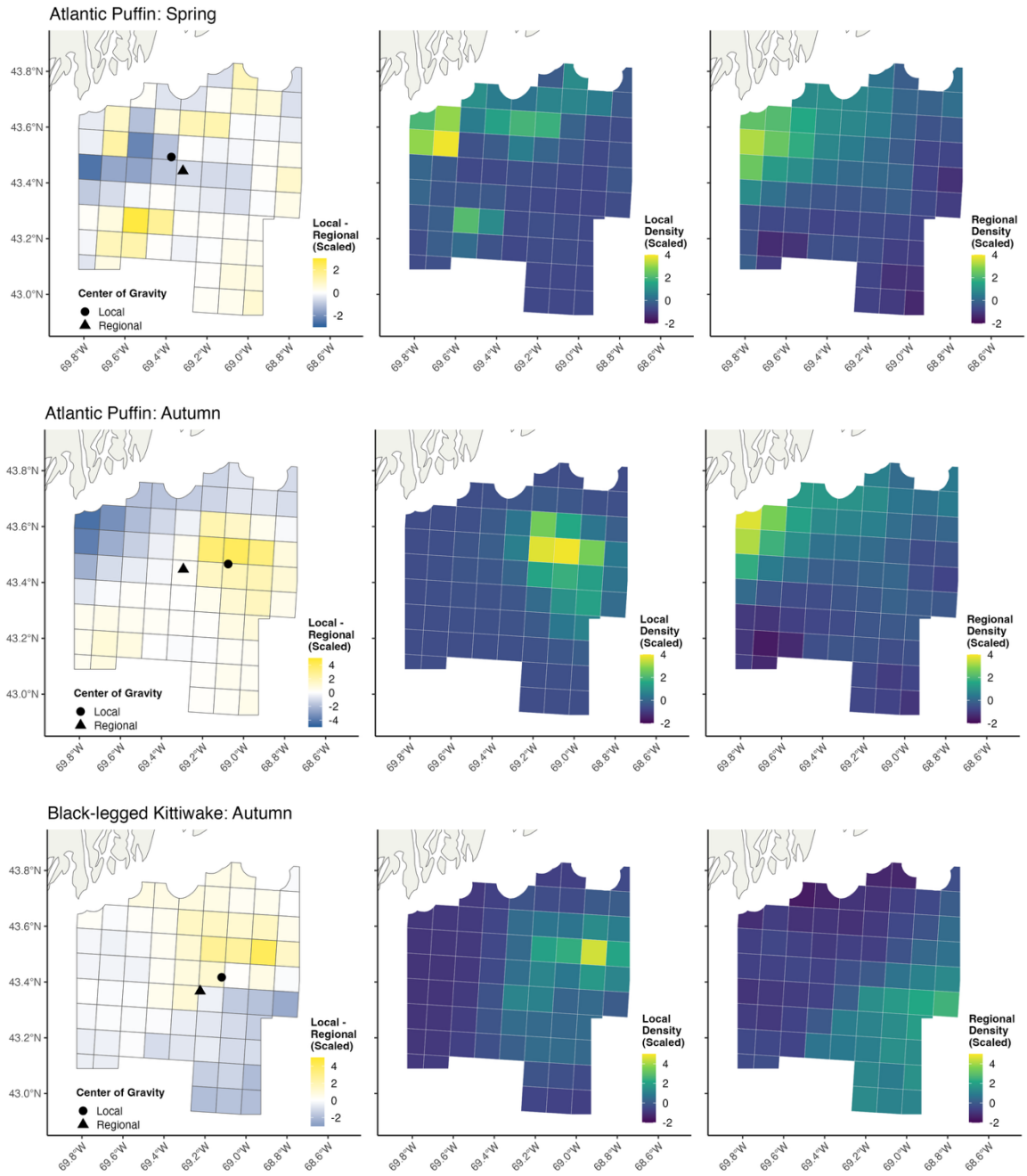
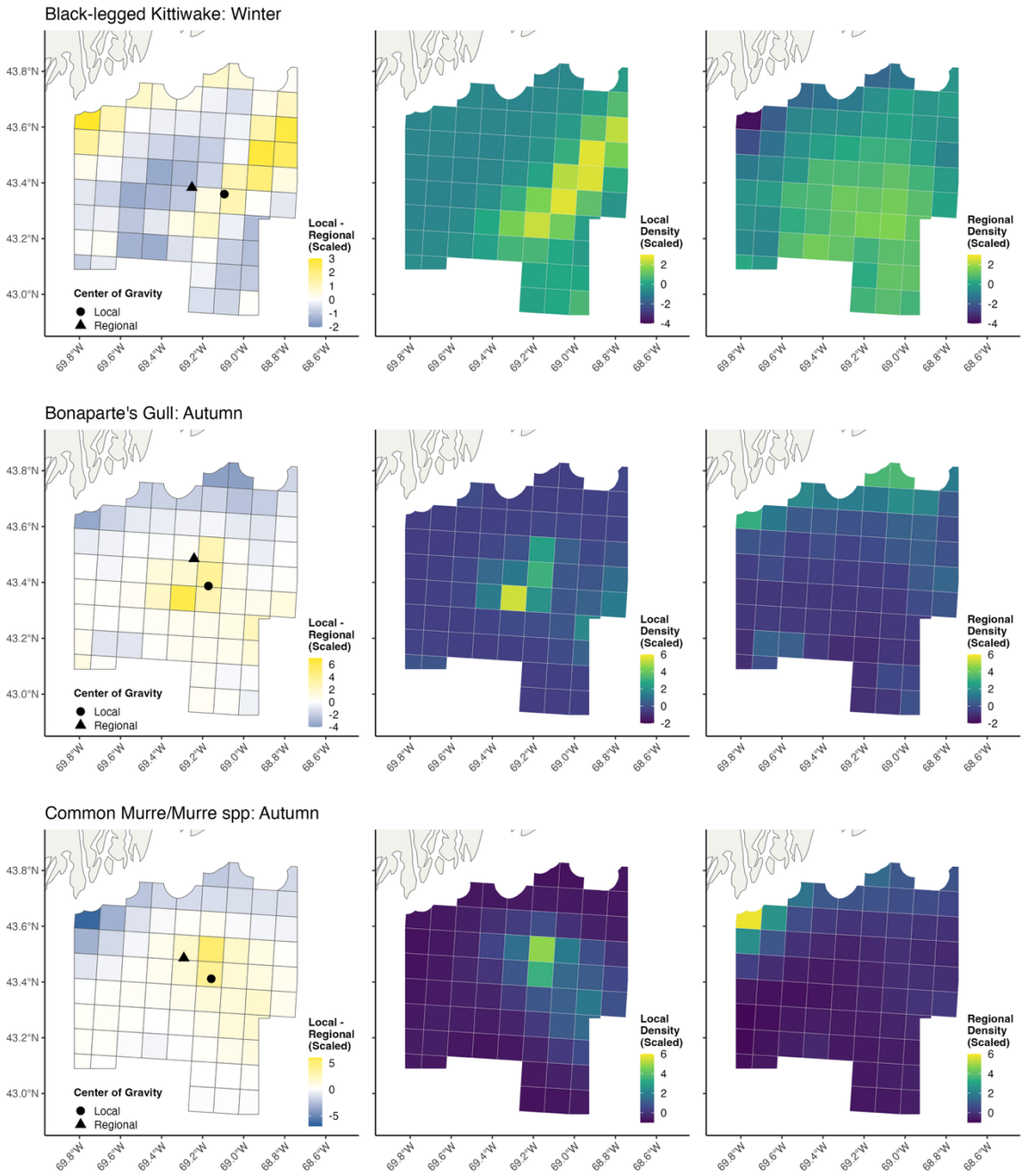
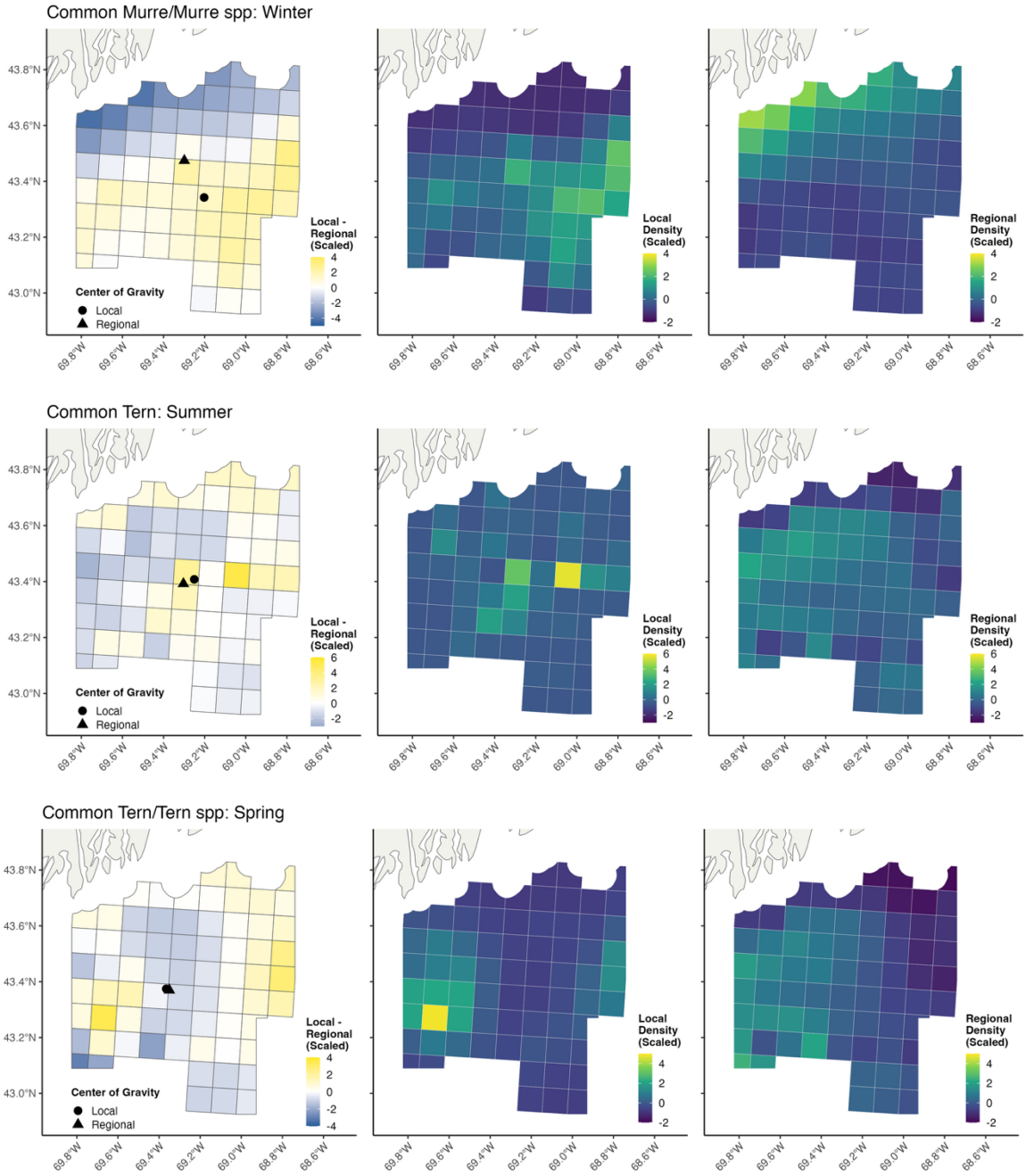
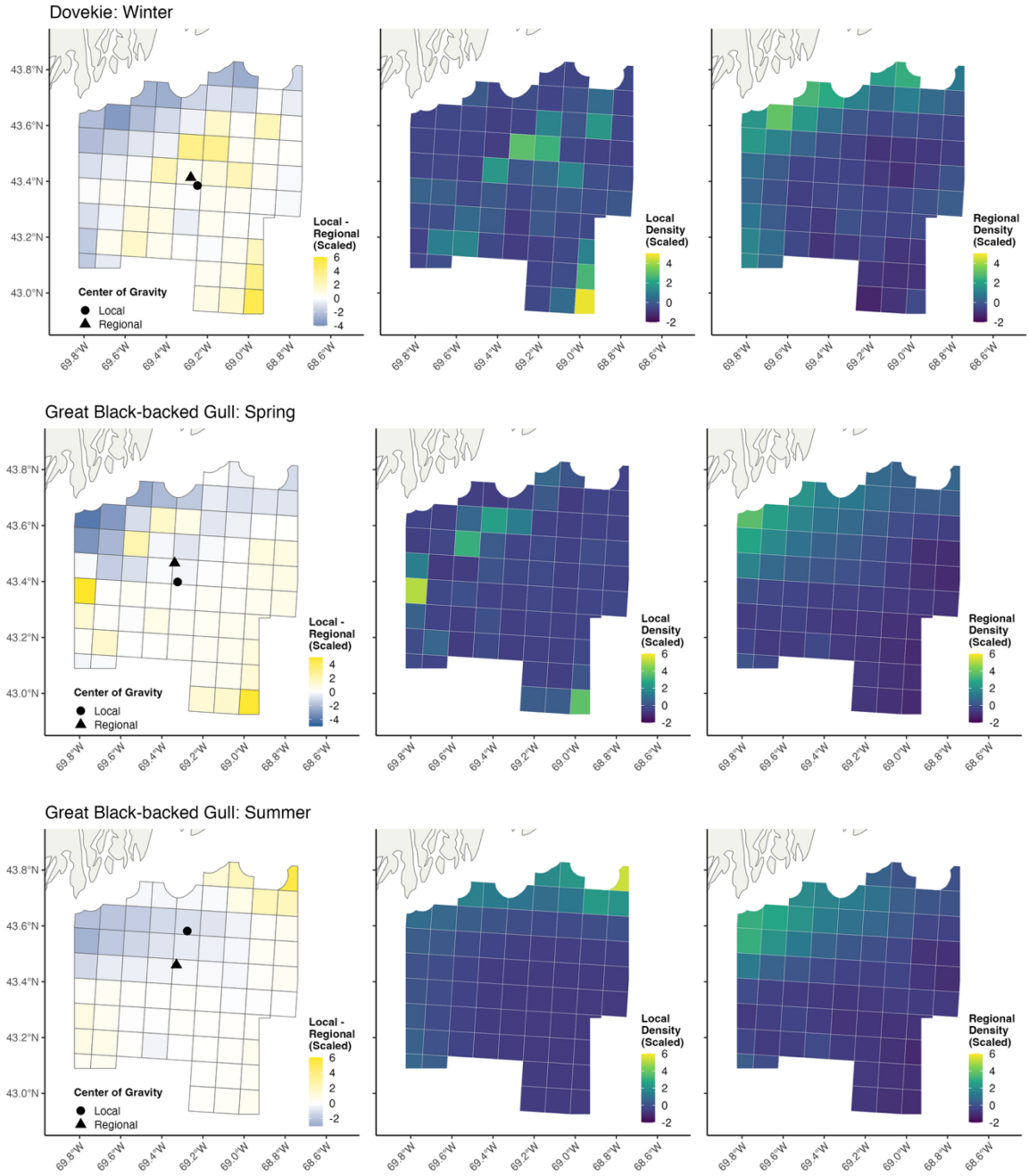


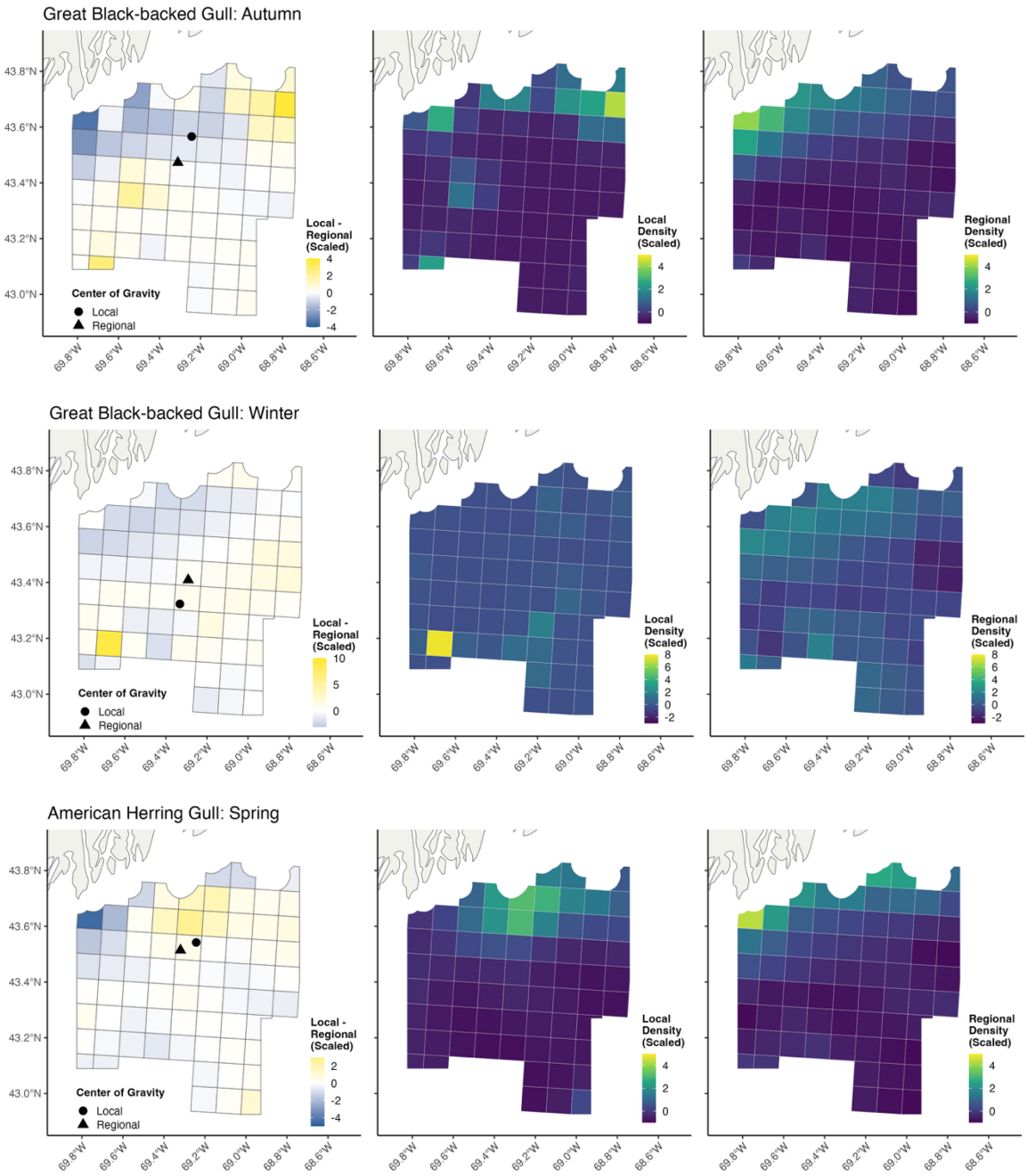
Figure A3. Global spatial cross-correlation indices (GSCI) of scaled local and regional density estimates for all taxon/season comparisons (*n* = 24) using inverse power weighting (left) for the distance between locations, and GSCIs of the local and regional coefficients of variation (CVs, *n* = 21) by inverse power weighting (center) and negative exponential weighting (right). The GSCI explains broadscale spatial cross-correlation between the two model density estimates/CVs across the entire Gulf of Maine study area. Index values can vary from –1 to 1; blues indicate values < 0 (negative correlations), yellows are values > 0 (positive correlations), and zero values are gray. Common names and alpha codes are on the vertical axis. CVs of multi-species groups were not compared (see Methods).

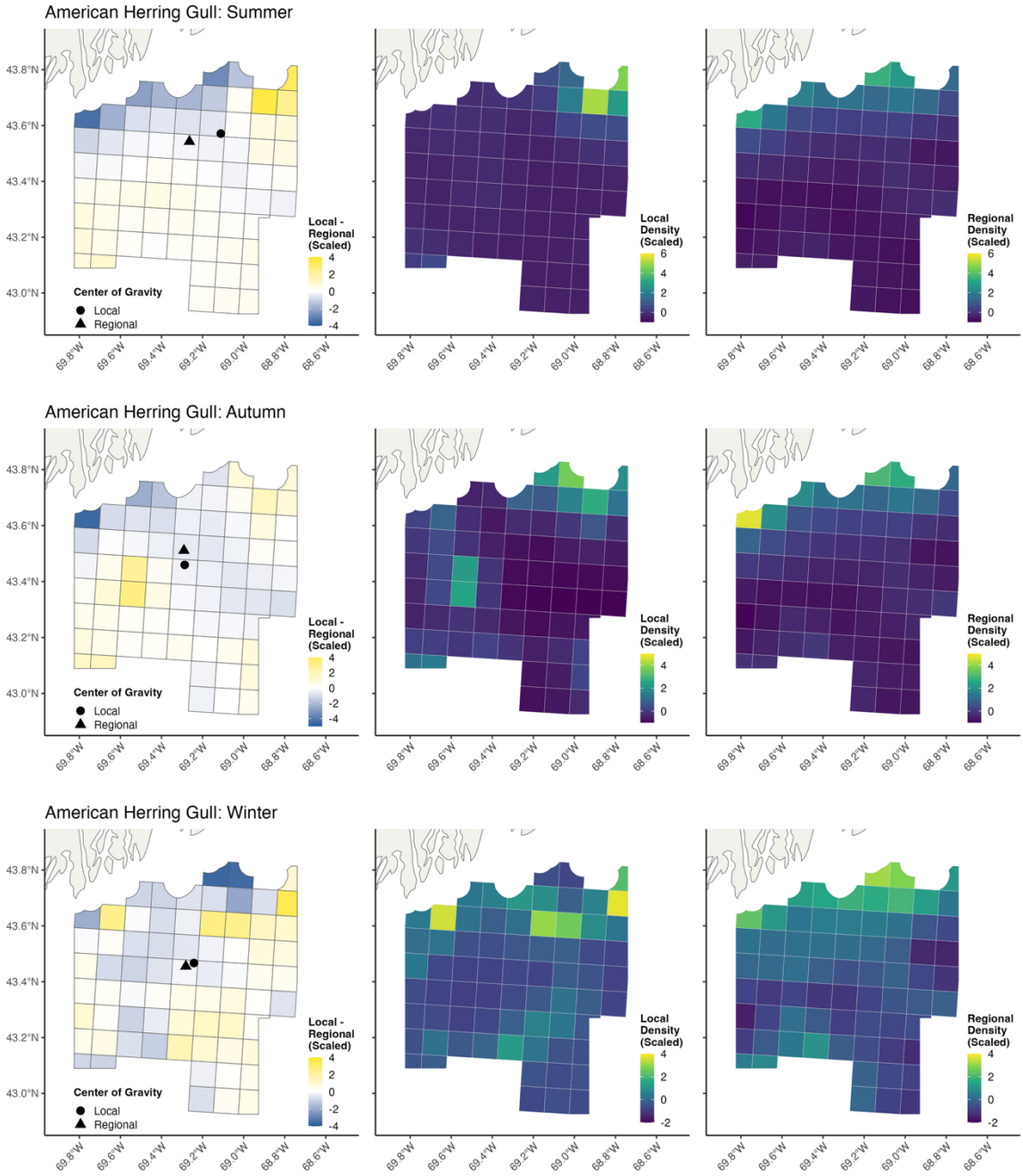

Atlantic Puffin: Spring
Local - Regional (Scaled)
Local Density (Scaled)
Regional Density (Scaled)
Center of Gravity
Local
Regional
Atlantic Puffin: Autumn
Black-legged Kittiwake: Autumn
43.8°N
43.6°N
43.4°N
43.2°N
43.0°N
69.8°W
69.6°W
69.4°W
69.2°W
69.0°W
68.8°W
68.6°W

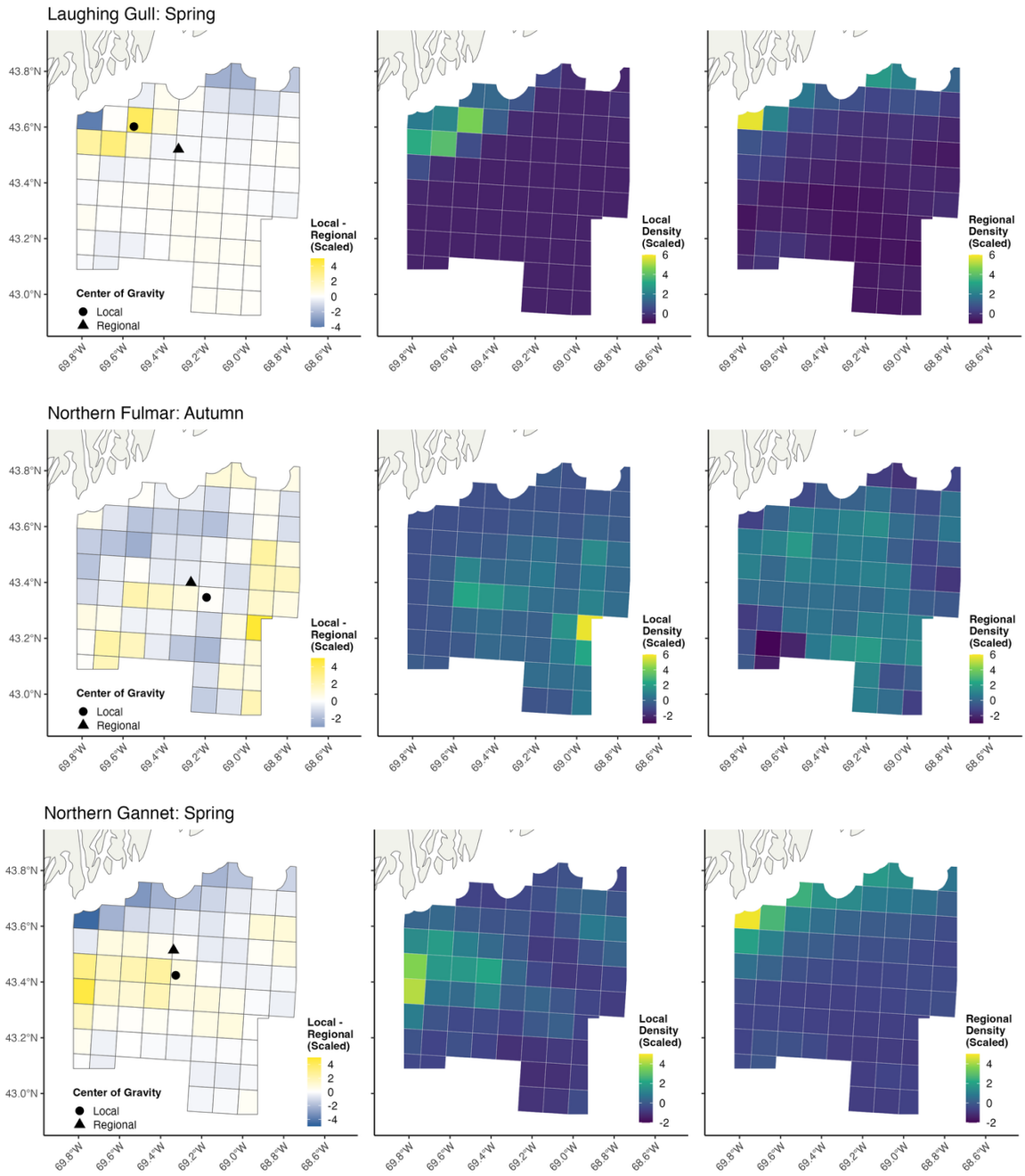

Black-legged Kittiwake: Winter
Bonaparte's Gull: Autumn
Common Murre/Murre spp: Autumn
Local - Regional (Scaled)
Local Density (Scaled)
Regional Density (Scaled)
Center of Gravity
Local
Regional
43.8°N
43.6°N
43.4°N
43.2°N
43.0°N
69.8°W
69.6°W
69.4°W
69.2°W
69.0°W
68.8°W
68.6°W


Common Murre/Murre spp: Winter
Common Tern: Summer
Common Tern/Tern spp: Spring
Local - Regional (Scaled)
Local Density (Scaled)
Regional Density (Scaled)
Center of Gravity
Local
Regional
43.8°N
43.6°N
43.4°N
43.2°N
43.0°N
69.8°W
69.6°W
69.4°W
69.2°W
69.0°W
68.8°W
68.6°W


Dovekie: Winter
Great Black-backed Gull: Spring
Great Black-backed Gull: Summer
Local - Regional (Scaled)
Local Density (Scaled)
Regional Density (Scaled)
Center of Gravity
Local
Regional
43.8°N
43.6°N
43.4°N
43.2°N
43.0°N
69.8°W
69.6°W
69.4°W
69.2°W
69.0°W
68.8°W
68.6°W


Great Black-backed Gull: Autumn
Great Black-backed Gull: Winter
American Herring Gull: Spring
Local - Regional (Scaled)
Local Density (Scaled)
Regional Density (Scaled)
Center of Gravity
Local
Regional
43.8°N
43.6°N
43.4°N
43.2°N
43.0°N
69.8°W
69.6°W
69.4°W
69.2°W
69.0°W
68.8°W
68.6°W


American Herring Gull: Summer
American Herring Gull: Autumn
American Herring Gull: Winter
Local - Regional (Scaled)
Local Density (Scaled)
Regional Density (Scaled)
Center of Gravity
Local
Regional
43.8°N
43.6°N
43.4°N
43.2°N
43.0°N
69.8°W
69.6°W
69.4°W
69.2°W
69.0°W
68.8°W
68.6°W


Laughing Gull: Spring
Northern Fulmar: Autumn
Northern Gannet: Spring
Local - Regional (Scaled)
Local Density (Scaled)
Regional Density (Scaled)
Center of Gravity
Local
Regional
43.8°N
43.6°N
43.4°N
43.2°N
43.0°N
69.8°W
69.6°W
69.4°W
69.2°W
69.0°W
68.8°W
68.6°W

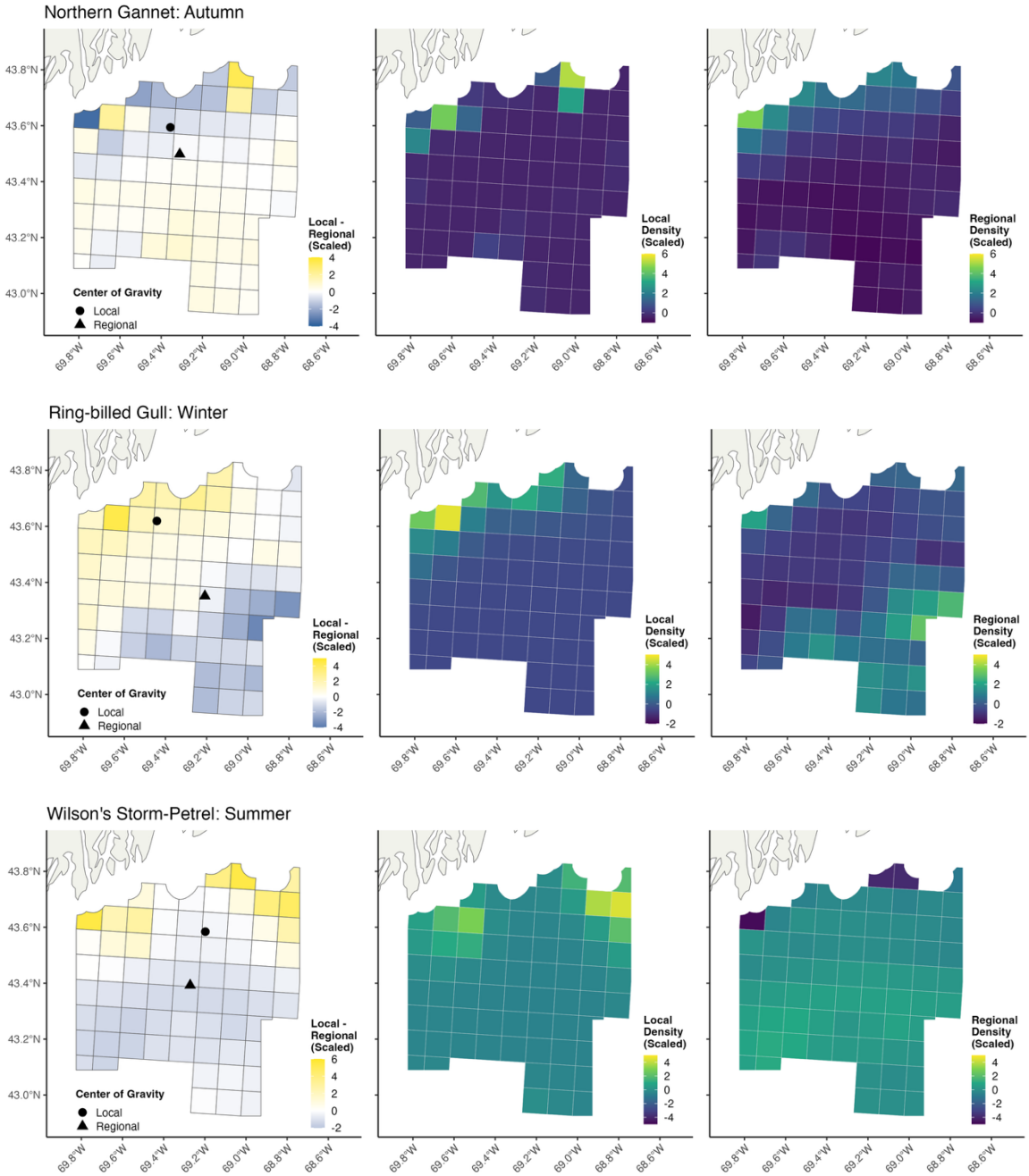
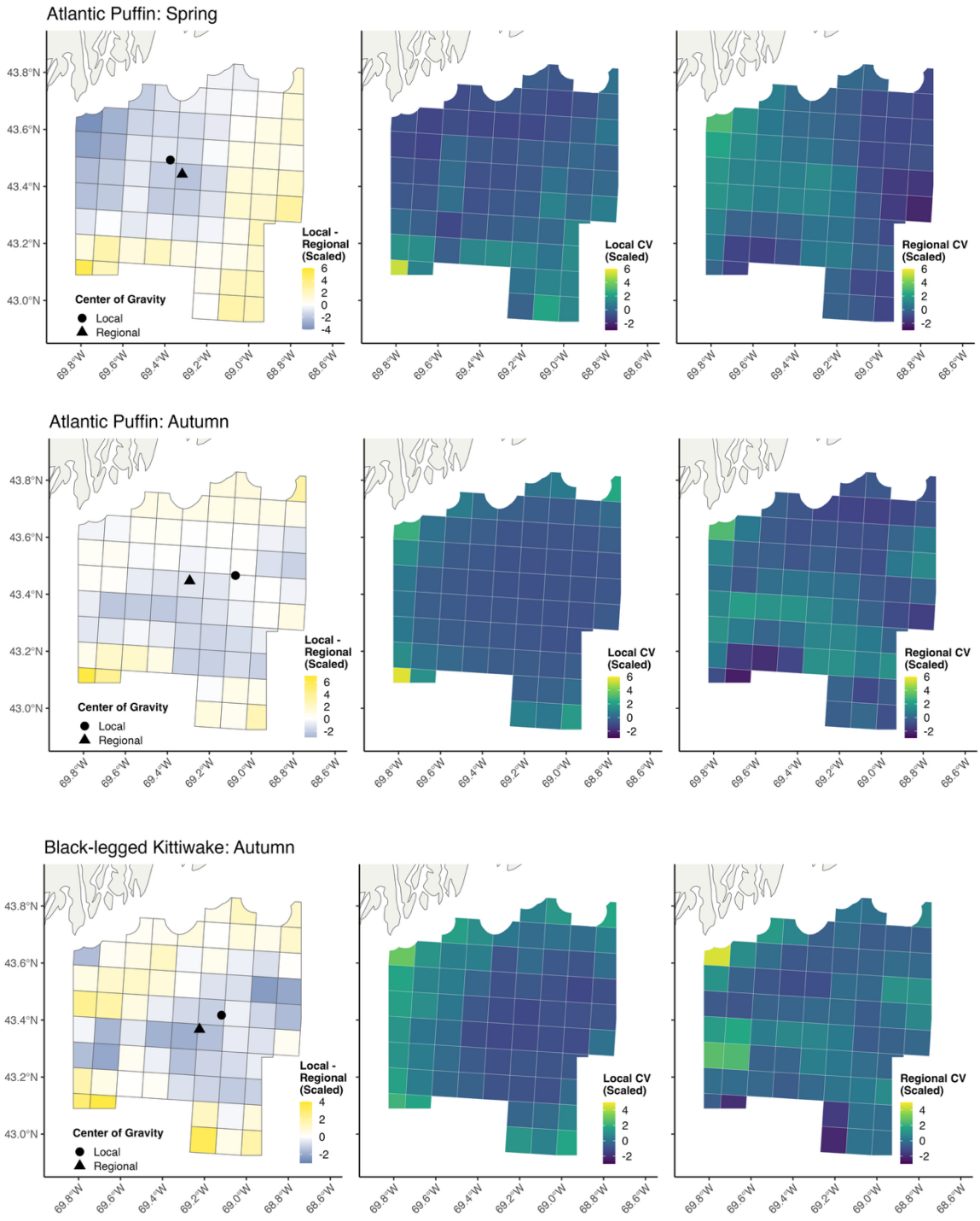
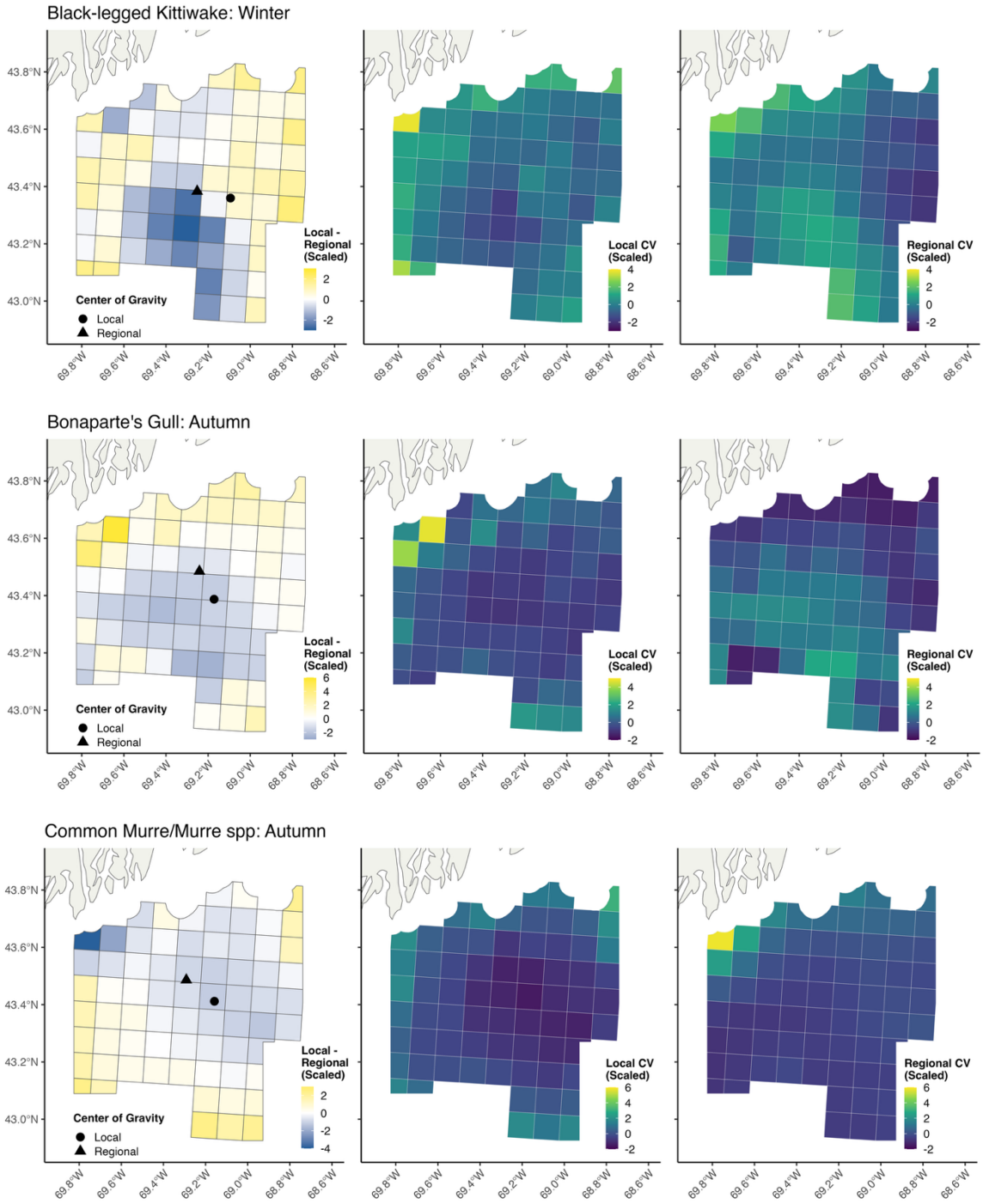
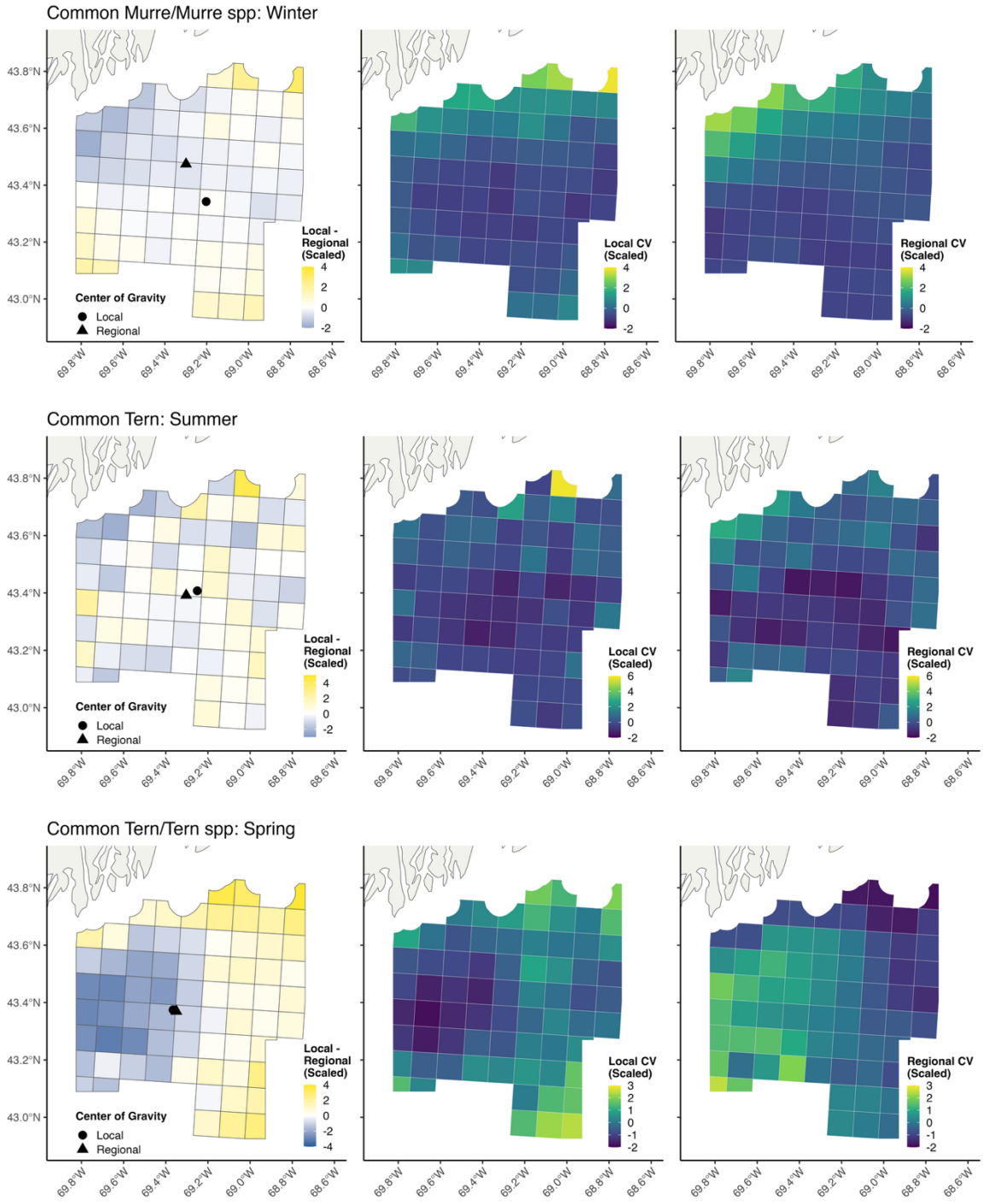
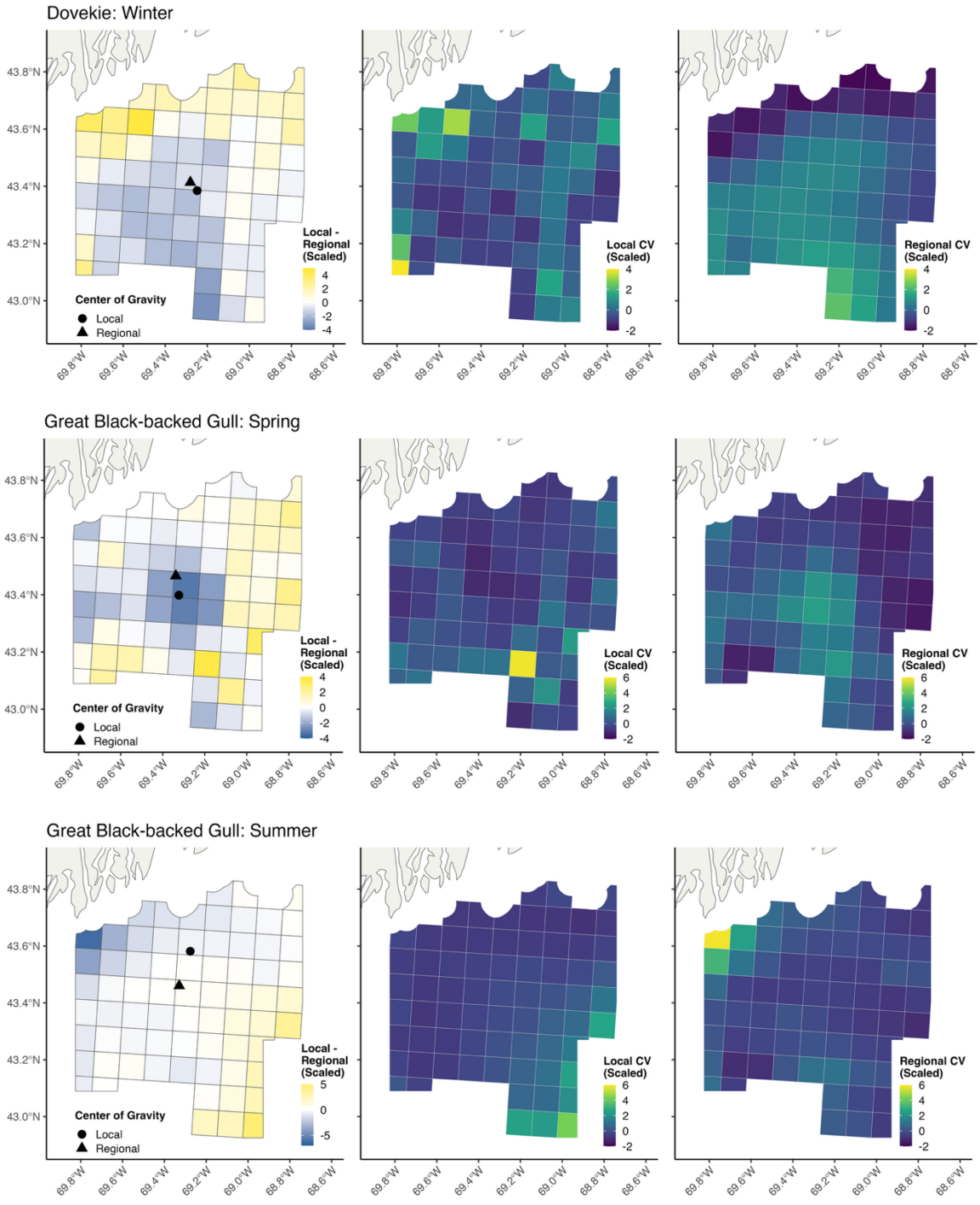


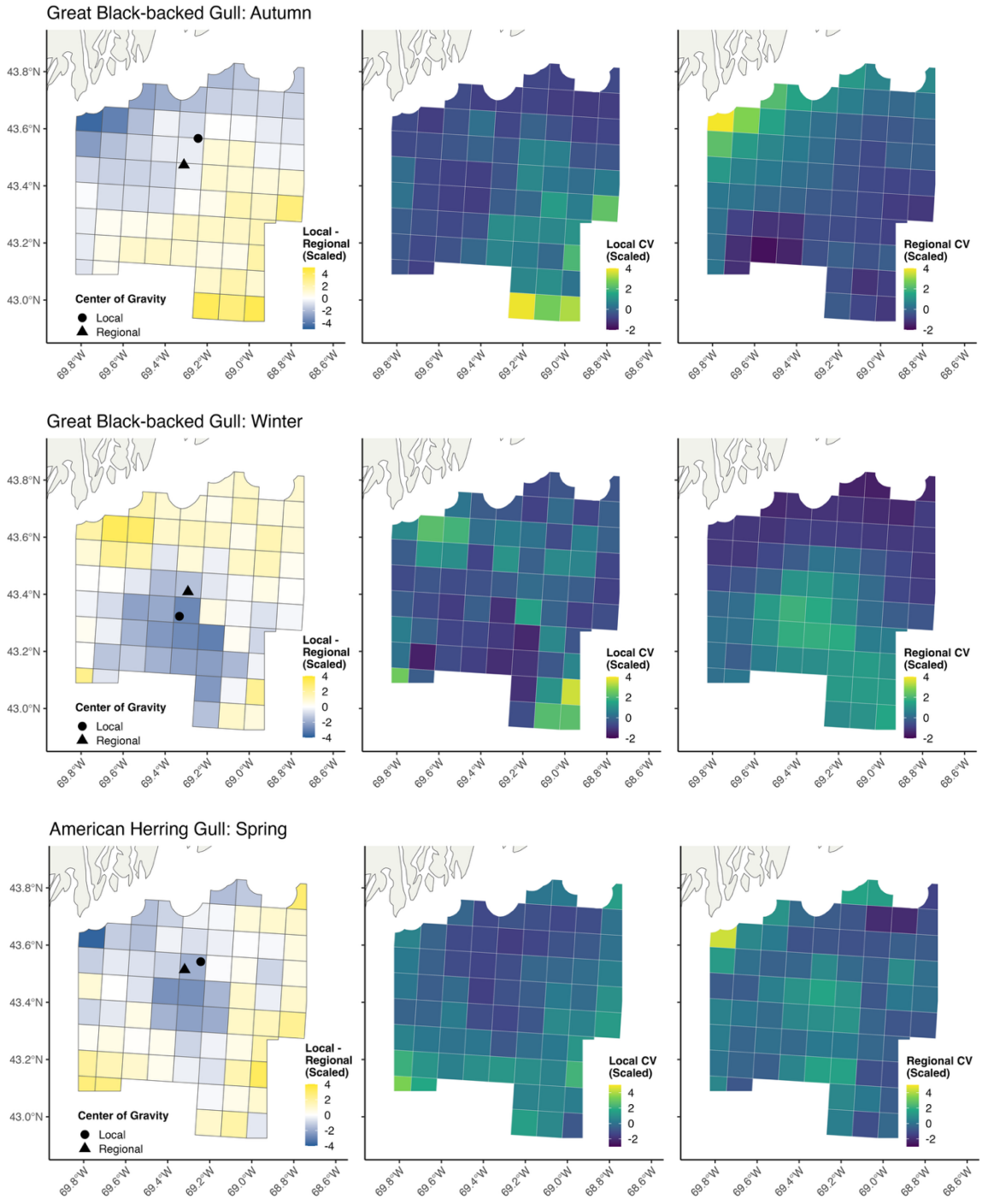
Figure A4. Scaled density maps for taxon and season comparisons between local and regional model predictions. Left panels show the centers of gravity and the absolute differences in scaled density values between the local and regional models (white: no difference between model values; yellow: local > regional value; blue: regional > local value). Center panels show the scaled values from the local model, and right panels show the scaled values from the regional model. Panel color scales are specific to each taxon/season combination (see each panel legend key).

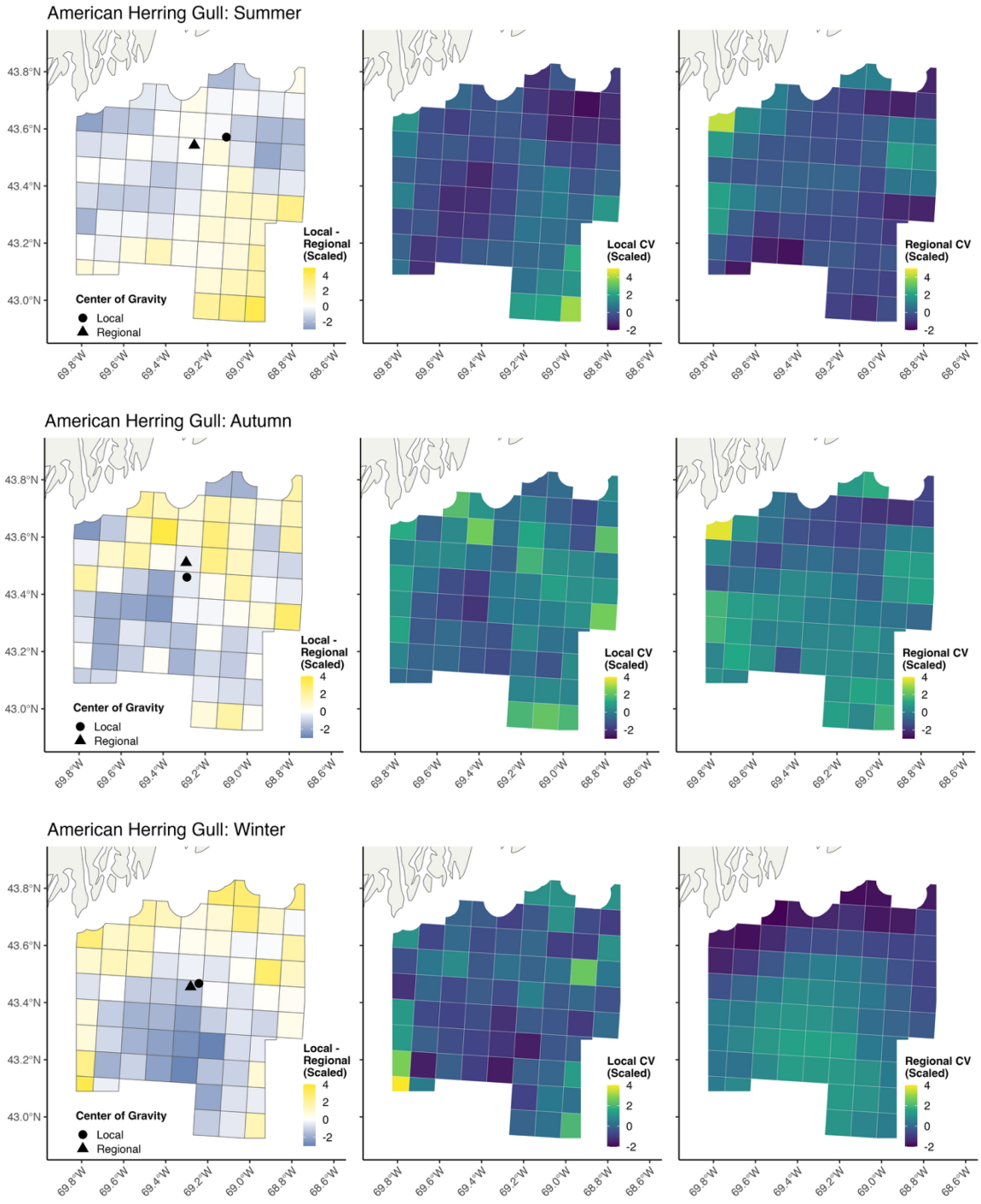

Atlantic Puffin: Spring
Local - Regional (Scaled)
Local CV (Scaled)
Regional CV (Scaled)
Center of Gravity
Local
Regional
Atlantic Puffin: Autumn
Local - Regional (Scaled)
Local CV (Scaled)
Regional CV (Scaled)
Center of Gravity
Local
Regional
Black-legged Kittiwake: Autumn
Local - Regional (Scaled)
Local CV (Scaled)
Regional CV (Scaled)
Center of Gravity
Local
Regional

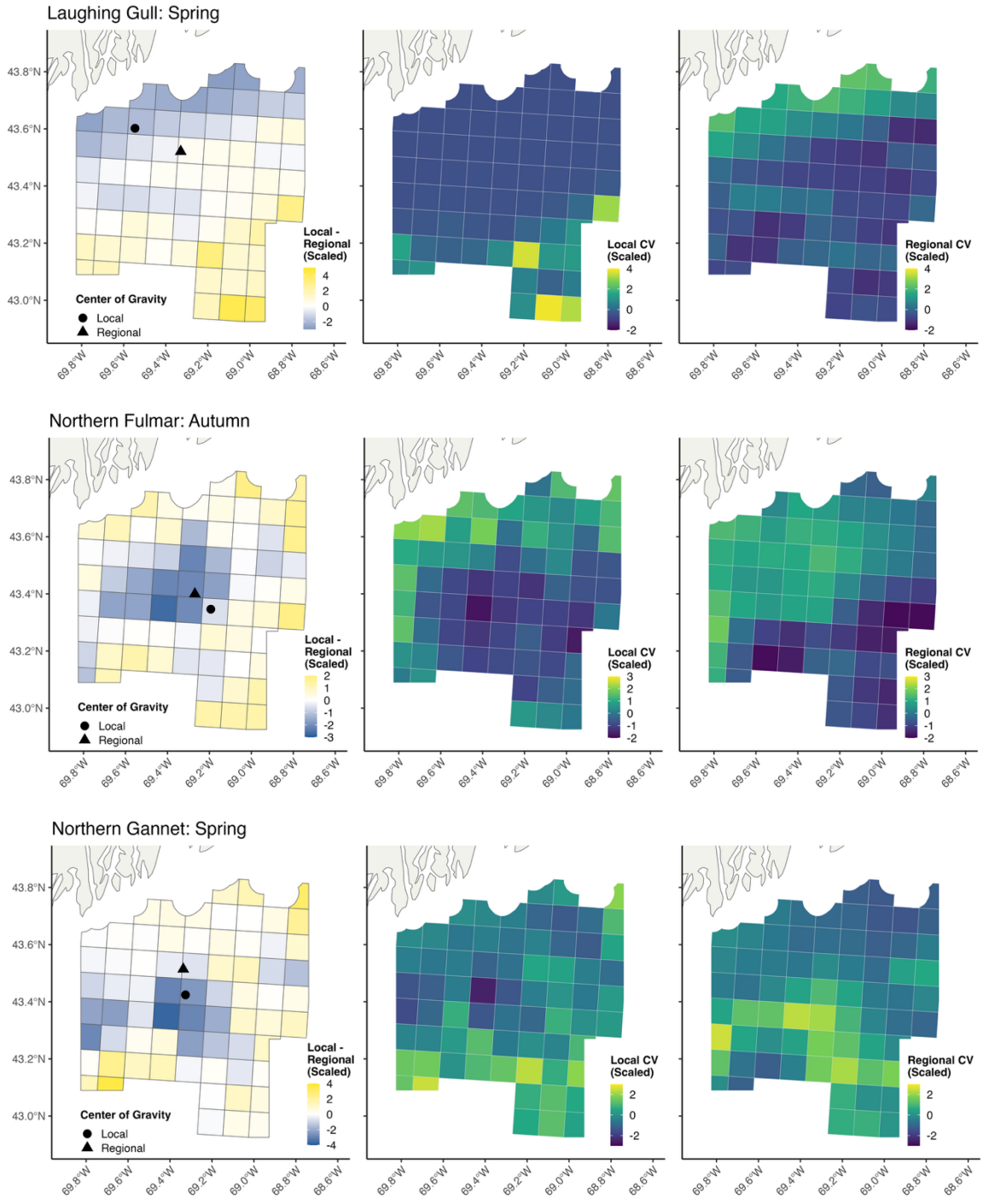

Black-legged Kittiwake: Winter
Bonaparte's Gull: Autumn
Common Murre/Murre spp: Autumn
Local - Regional (Scaled)
Local CV (Scaled)
Regional CV (Scaled)
Center of Gravity
Local
Regional
43.8°N
43.6°N
43.4°N
43.2°N
43.0°N
69.8°W
69.6°W
69.4°W
69.2°W
69.0°W
68.8°W
68.6°W


Common Murre/Murre spp: Winter
Common Tern: Summer
Common Tern/Tern spp: Spring
Local - Regional (Scaled)
Local CV (Scaled)
Regional CV (Scaled)
Center of Gravity
Local
Regional
43.8°N
43.6°N
43.4°N
43.2°N
43.0°N
69.8°W
69.6°W
69.4°W
69.2°W
69.0°W
68.8°W
68.6°W


Dovekie: Winter
Great Black-backed Gull: Spring
Great Black-backed Gull: Summer
Local - Regional (Scaled)
Local CV (Scaled)
Regional CV (Scaled)
Center of Gravity
Local
Regional
43.8°N
43.6°N
43.4°N
43.2°N
43.0°N
69.8°W
69.6°W
69.4°W
69.2°W
69.0°W
68.8°W
68.6°W


Great Black-backed Gull: Autumn
Great Black-backed Gull: Winter
American Herring Gull: Spring
Local - Regional (Scaled)
Local CV (Scaled)
Regional CV (Scaled)
Center of Gravity
Local
Regional
43.8°N
43.6°N
43.4°N
43.2°N
43.0°N
69.8°W
69.6°W
69.4°W
69.2°W
69.0°W
68.8°W
68.6°W


American Herring Gull: Summer
American Herring Gull: Autumn
American Herring Gull: Winter
Local - Regional (Scaled)
Local CV (Scaled)
Regional CV (Scaled)
Center of Gravity
Local
Regional
43.8°N
43.6°N
43.4°N
43.2°N
43.0°N
69.8°W
69.6°W
69.4°W
69.2°W
69.0°W
68.8°W
68.6°W
4
2
0
-2


Laughing Gull: Spring
Local - Regional (Scaled)
Local CV (Scaled)
Regional CV (Scaled)
Center of Gravity
Local
Regional
Northern Fulmar: Autumn
Local - Regional (Scaled)
Local CV (Scaled)
Regional CV (Scaled)
Center of Gravity
Local
Regional
Northern Gannet: Spring
Local - Regional (Scaled)
Local CV (Scaled)
Regional CV (Scaled)
Center of Gravity
Local
Regional

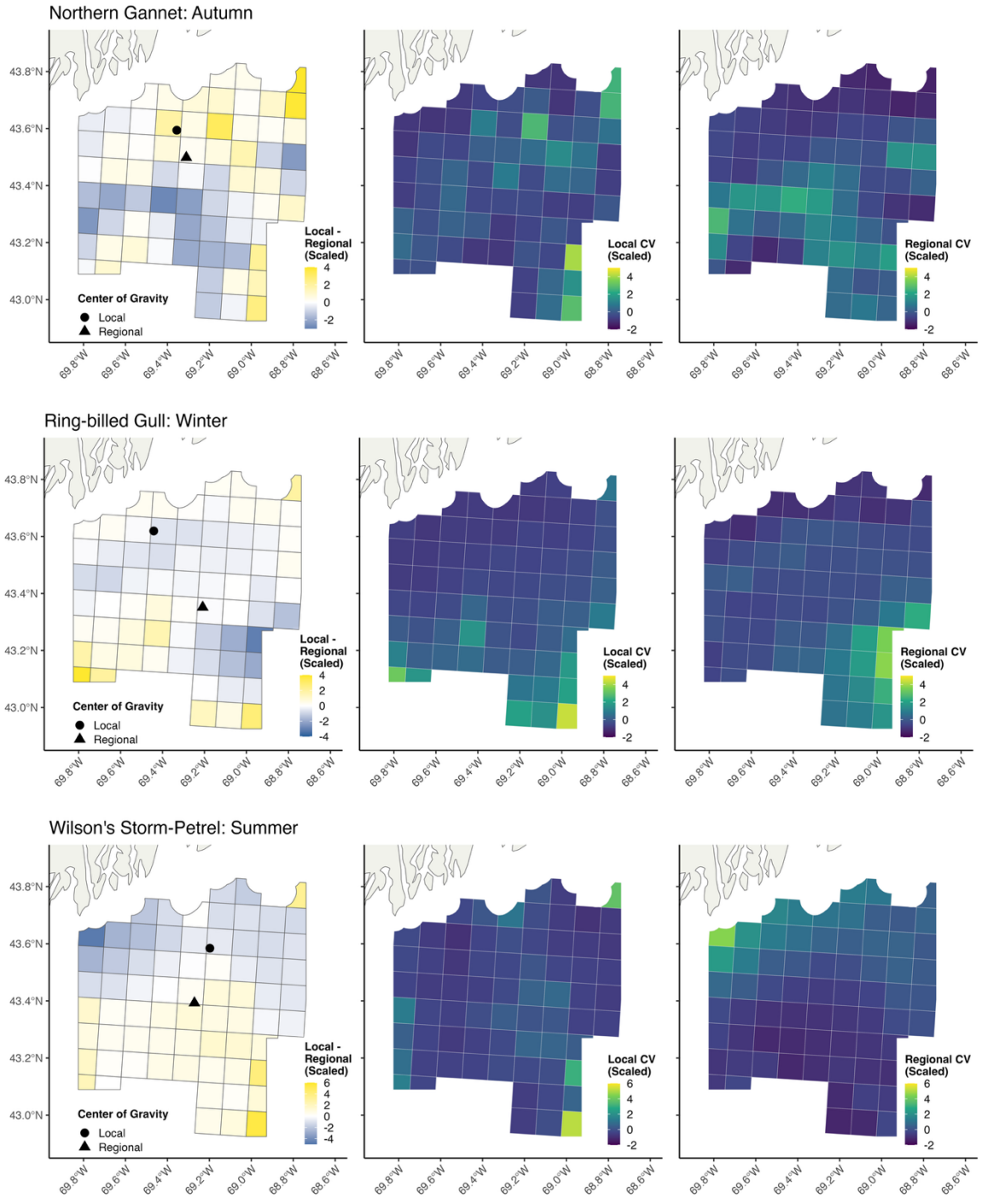


Figure A5. Scaled coefficient of variation (CV) maps for species and season comparisons between local and regional models. Left panels show the centers of gravity and the absolute differences in scaled CVs between the local and regional models (white: no difference between model values; yellow: local > regional value; blue: regional > local value). Center panels show the scaled CV values from the local model, and right panels show the scaled CV values from the regional model. Panel color scales are specific to each taxon/season combination (see each panel legend key).

Literature Cited

Burke CM, Montevecchi WA (2018) Taking the bite out of winter: Common Murres (*Uria aalge*) push their dive limits to surmount energy constraints. Front Mar Sci 5.

Cairns DK, Bredin KA, Montevecchi WA (1987) Activity budgets and foraging ranges of breeding Common Murres. Auk 104: 218–224.

Coleman K, Dettloff K, Jones M, Wimer M, Bigger D (2016) The Northwest Atlantic Seabird Catalog: How an aggregation of seabird observations is informing policy decisions.

Dunn RE, Duckworth J, O'Brien S, Furness RW, Buckingham L, Daunt F, Bogdanova M, Green JA (2024) Temporal and spatial variability in availability bias has consequences for marine bird abundance estimates during the non-breeding season. Ecol Sol and Evidence 5: e12373.

Gjerdrum C, Fifield DA, Wilhelm SI (2012) Eastern Canada Seabirds at Sea (ECSAS) Standardized Protocol for Pelagic Seabird Surveys from Moving and Stationary Platforms. Canadian Wildlife Service, Atlantic Region. vi + 37 pp.

Halpin PN, Read AJ, Fujioka E, Best BD, Donnelly B, Hazen LJ, Kot C, Urian K, LaBrecque E, DiMatteo A, Cleary J, Good C, Crowder LB, Hyrenbach KD (2009) OBIS-SEAMAP: The world data center for marine mammal, sea bird, and sea turtle distributions. Oceanography 22: 104–115.

Karnovsky N, Brown Z, Welcker J, Harding A, Walkusz W, Cavalcanti A, Hardin J, Kitaysky A, Gabrielsen G, Grémillet D (2011) Inter-colony comparison of diving behavior of an Arctic top predator: implications for warming in the Greenland Sea. Mar Ecol Prog Ser 440: 229–240.

O'Connell AF, Gardner AT, Gilbert AT, Laurent K (2009) Compendium of Avian Occurrence Information for the Continental Shelf Waters along the Atlantic Coast of the United States, Final Report (Database Section - Seabirds). OCS Study BOEM 2012-076. Prepared by the USGS Patuxent Wildlife Research Center.

Spencer SM (2012) Diving Behavior and Identification of Sex of Breeding Atlantic Puffins (*Fratercula arctica*), and Nest-Site Characteristics of Alcids on Petit Manan Island, Maine. University of Massachusetts, Amherst.

Winship A, Leirnes J, Coyne M, Howell J, Saba V, Christensen J (2023) Modeling the Distributions of Marine Birds at Sea to Inform Planning of Energy Development on the US Atlantic Outer Continental Shelf. Report No.: OCS Study BOEM 2023-060. Department of the Interior, Bureau of Ocean Energy Management, Sterling Virginia, USA. 413 p.